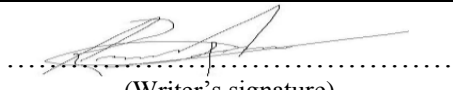




University of  
Stavanger

Faculty of Science and Technology

## MASTER'S THESIS

Study program/ Specialization: Petroleum Engineering/Production	Spring semester, 2012  <u>Open</u> / Restricted access
Writer: Rodrigo Aguilar Ruyschaert	 (Writer's signature)
Faculty supervisor: Aly A. Hamouda External supervisor(s): Arild Aarskog	
Title of thesis:  "Optimization of the Lift Gas Compression System at the Eldfisk Complex"	
Credits (ECTS): 30	
Key words: VLP IPR Theoretical Optimum Lift Gas injection Economical Optimum Lift Gas injection Compression System Insufficient Pressure High Recirculation	Pages: 57  + enclosure: Appendix A (17) Appendix B (8)  Stavanger, 14/06/2012 Date/year

UNIVERSITY OF STAVANGER IN COOPERATION WITH CONOCOPHILLIPS



# Optimization of the Lift Gas Compression System at the Eldfisk Complex

---

**Rodrigo Aguilar Ruysschaert**

**June, 2012**

A THESIS SUBMITTED TO THE  
UNIVERSITY OF STAVANGER  
IN FULFILLMENT OF THE REQUIREMENTS  
FOR THE DEGREE OF:

MASTER OF SCIENCE IN PETROLEUM ENGINEERING

## Abstract

The intention of this study was to maximize the oil production of the Eldfisk field. Two major constraints were encountered limiting the amount of gas that can be injected into the wells. Optimizing production taking these constraints into consideration will thus maximize production. A MatLab code has been developed for this work and 18 wells of the Eldfisk field have been simulated to compute the optimum gas lift injection rate. Given the limitations the economic optimum has been estimated from the gas lift performance curve of every well.

The economic optimum has been calculated for the actual conditions of the field and also for a scenario with a higher water cut, corresponding to future operation.

The results of the economic lift gas injection rate were used as input data for a HYSYS case, with the objective to optimize the compression system on Eldfisk 2/7 E. Three aspects of the compression system were of main concern: insufficient discharge pressure, high recirculation rates and low efficiency of the third stage of compression

To optimize the compression system, different scenarios were evaluated with the objective to find the best scenario for the discovered issues. One solution was found that allowed all of the issues previously mentioned to be covered successfully simultaneously.

By reducing the speed of the compressors, the discharge point for lift gas was moved from the second to the third compression stage, also the pressure for gas lift wells was increased to the specified range and the recirculation rates were decreased so the scrubbers will not be working to their limit capacity, finally with these modification the overall power consumption was reduced.

## Acknowledgments

I would like to express my deepest gratitude to my faculty supervisor, Aly Hamouda, for his excellent guidance and support given throughout writing this thesis, I am sure it would have not been possible without his help.

I owe sincere and deep thankfulness to my external supervisor from ConocoPhillips Norge, Arild Aarskog, who gave me the opportunity to work in such an exciting topic; the support and countless conversations were key factors that helped putting together all the ideas and finally the project.

Gratitude is also extended to ConocoPhillips Norge for giving me the opportunity to be part of one of the most important oil companies as a graduate engineer, and for sharing with me all the necessary data to carry out this project.

I would also like to thank my mother, my grandmother, my brother, and in general all my family because even though the big distances they were always supporting me and encouraging me with their best wishes and love.

Finally, I would like to thank my girlfriend, Angeliki, for her love and support through the good and bad times.

## Table of Contents

Abstract .....	ii
Acknowledgments.....	iii
Table of Contents .....	iv
List of Figures .....	vi
List of Tables .....	viii
Chapter 1. Introduction .....	1
1.1. Overview .....	1
1.2. Problem Statement .....	3
1.3. Objectives.....	4
Chapter 2. Methodology .....	5
Chapter 3. Gas Lift Theory .....	6
3.1. Introduction .....	6
3.2. Gas Lift System.....	6
3.3. Inflow Performance Relationship (IPR).....	9
3.4. Vertical Lift Performance (VLP) .....	11
3.5. Beggs and Brill Model .....	12
3.6. Review of Gas Properties and Equation of State (EOS).....	19
3.7. Gas Lift Performance Curve .....	21
Chapter 4. Compression Theory .....	24
4.1 Introduction .....	24
4.2 Types of compressors.....	24
4.3 Staged compression.....	26
4.4 Operating Parameters .....	27
4.5 Anti-Surge Systems.....	27
4.6 Prime Drivers .....	28

Chapter 5. Results and Discussions .....	30
5.1. Gas Lift Volume.....	30
5.1.1 Optimum Gas Lift Injection Rate .....	31
5.1.2 Economic Optimum Gas Lift Injection Rate .....	34
5.2 Optimization of the compression train .....	39
Chapter 6. Conclusions .....	45
References.....	46
Nomenclature.....	49
Appendix A – Graphic results of the Simulations .....	50
Appendix B – Gas Lift Performance Curves .....	67

## List of Figures

Figure 1.1: Eldfisk Complex.....	2
Figure 1.2: Simplified Process Flow Diagram of the Gas Compression System .....	3
Figure 3.1: Configuration of a typical gas lift well.....	7
Figure 3.2: VLP & IPR curves.....	9
Figure 3.3: Typical Inflow Performance Curves .....	10
Figure 3.4: Flow Regimes Identified by Beggs and Brill .....	13
Figure 3.5: Beggs and Brill Process flow Diagram .....	18
Figure 3.6: VLP curves for increasing gas injection rate.....	22
Figure 3.7: Gas Lift Performance Curve.....	22
Figure 4.1: Typical Compression Stage.....	24
Figure 4.2: Operating envelope for centrifugal and reciprocating compressors.....	25
Figure 4.3: Typical Compressor Operating Curves. ....	27
Figure 5.1: Method proposed to calculate the theoretical optimum .....	31
Figure 5.2: VLP curves for Well A-06 .....	32
Figure 5.3: VLP vs. IPR for well A-06.....	32
Figure 5.4: Gas Lift Performance Curve for Well A-06.....	34
Figure 5.5: Gas Lift Performance Curve for Well B-10 .....	35
Figure 5.6: A comparison of the Results obtained.....	37
Figure 5.7: Modified Operating conditions in typical compression head curves .....	40
Figure 5.8: Compression Train – First Stage.....	41
Figure 5.9: Compression Train – Second Stage.....	42
Figure 5.10: Compression Train – Third Stage .....	43
Figure A-1: VLP curves for Well A-01 .....	50
Figure A-2: VLP vs. IPR for well A-01.....	50
Figure A-3: VLP curves for Well A-02 .....	51
Figure A-4: VLP vs. IPR for well A-02.....	51
Figure A-5: VLP curves for Well A-03 .....	52
Figure A-6: VLP vs. IPR for well A-03.....	52
Figure A-7: VLP curves for Well A-10 .....	53
Figure A-8: VLP vs. IPR for well A-10.....	53
Figure A-9: VLP curves for Well A-16 .....	54
Figure A-10: VLP vs. IPR for well A-16.....	54
Figure A-11: VLP curves for Well A-17 .....	55
Figure A-12: VLP vs. IPR for well A-17.....	55
Figure A-13: VLP curves for Well A-18 .....	56
Figure A-14: VLP vs. IPR for well A-18.....	56
Figure A-15: VLP curves for Well A-19 .....	57
Figure A-16: VLP vs. IPR for well A-19.....	57
Figure A-17: VLP curves for Well A-20 .....	58
Figure A-18: VLP vs. IPR for well A-20.....	58
Figure A-19: VLP curves for Well A-23 .....	59

Figure A-20: VLP vs. IPR for well A-23.....	59
Figure A-21: VLP curves for Well A-26.....	60
Figure A-22: VLP vs. IPR for well A-26.....	60
Figure A-23: VLP curves for Well A-28.....	61
Figure A-24: VLP vs. IPR for well A-28.....	61
Figure A-25: VLP curves for Well B-10.....	62
Figure A-26: VLP vs. IPR for well B-10.....	62
Figure A-27: VLP curves for Well B-11.....	63
Figure A-28: VLP vs. IPR for well B-11.....	63
Figure A-29: VLP curves for Well B-14.....	64
Figure A-30: VLP vs. IPR for well B-14.....	64
Figure A-31: VLP curves for Well B-17.....	65
Figure A-32: VLP vs. IPR for well B-17.....	65
Figure A-33: VLP curves for Well B-19.....	66
Figure A-34: VLP vs. IPR for well B-19.....	66
Figure B-1: Gas Lift Performance Curve for Well A-01.....	67
Figure B-2: Gas Lift Performance Curve for Well A-02.....	67
Figure B-3: Gas Lift Performance Curve for Well A-03.....	68
Figure B-4: Gas Lift Performance Curve for Well A-10.....	68
Figure B-5: Gas Lift Performance Curve for Well A-16.....	69
Figure B-6: Gas Lift Performance Curve for Well A-17.....	69
Figure B-7: Gas Lift Performance Curve for Well A-18.....	70
Figure B-8: Gas Lift Performance Curve for Well A-19.....	70
Figure B-9: Gas Lift Performance Curve for Well A-20.....	71
Figure B-10: Gas Lift Performance Curve for Well A-23.....	71
Figure B-11: Gas Lift Performance Curve for Well A-26.....	72
Figure B-12: Gas Lift Performance Curve for Well A-28.....	72
Figure B-13: Gas Lift Performance Curve for Well B-11.....	73
Figure B-14: Gas Lift Performance Curve for Well B-14.....	73
Figure B-15: Gas Lift Performance Curve for Well B-17.....	74
Figure B-16: Gas Lift Performance Curve for Well B-19.....	74



## List of Tables

Table 2.1: Methodology Used in the present thesis .....	5
Table 3.1: Beggs and Brill Holdup constants .....	16
Table 4.1: Comparison between the main types of compressors .....	26
Table 5.1: Summary of the optimum injection and oil .....	33
Table 5.2: Summary of the economic optimum injection.....	36
Table 5.3: Summary of the economic optimum injection and oil production .....	38
Table 5.4: Proposed Scenarios and Results for First Compression Stage .....	41
Table 5.5: Proposed Scenarios and Results for second Compression Stage.....	42
Table 5.6: Proposed Scenarios and Results for Third Compression Stage.....	42
Table 5.7: Comparison of the total power consumption.....	43

## Chapter 1. Introduction

### 1.1.Overview

Eldfisk is an oil field located south of Ekofisk, in the southern part of the North Sea. The water depth in the area is 70 - 75metres. (ConocoPhillips, 2012) <sup>(1)</sup>

The Eldfisk field produces from the Ekofisk, Tor and Hod formations from the Early Paleocene and Late Cretaceous ages. The reservoir rock is fine-grained and dense, but with high porosity. The field consists of three structures: Alpha (A), Bravo (B) and East (E) Eldfisk. The reservoir lies at a depth of 2 700 - 2 900 meters. (ConocoPhillips, 2012) <sup>(1)</sup>

Eldfisk Field was originally developed by pressure depletion. In 1999, water injection began at the field, based on horizontal injection wells. The main artificial method used for oil recovery in the Eldfisk field is gas lift. Gas is also injected in periods when export is not possible. Pressure depletion has caused compaction in the reservoir, which has resulted in a few meters of seabed subsidence. (NPD, 2012) <sup>(2)</sup>

Eldfisk is developed with a total of four platforms. (ConocoPhillips, 2012) <sup>(1)</sup>

- Eldfisk A and Eldfisk FTP are wellhead facilities connected by a bridge. Eldfisk A also has drilling facilities. In 1999, a new water injection facility was integrated.
- Eldfisk E is a processing facility comprising the gas compression system and water injection. The facility also supplies the Ekofisk field with some injection water through a pipeline from Eldfisk to Ekofisk K.
- Eldfisk B is a combined drilling, wellhead and process facility located six kilometers northwest of the Eldfisk Complex.
- The Embla field, located south of Eldfisk, transports oil and gas via a 5.2 kilometer pipeline to Eldfisk FTP.
- In the future a new platform 2/7S will be installed at the Eldfisk center.



Figure 1.1: Eldfisk Complex. (ConocoPhillips, 2012) <sup>(1)</sup>

The multiphase flow coming from the wells is first separated in a production separator. The products from this process are: wet gas, oil and water.

After the Production separator the wet gas is divided into two streams, the first one goes to the Ekofisk center together with wet gas coming from Eldfisk 2/7B, the second stream goes to the gas compression system on Eldfisk 2/7E.

The gas compression system is composed of a three stage compression train, driven by a gas turbine. Before entering the first stage compressor the gas goes by a cooler and a scrubber in order to remove all possible condensable components and to protect all rotating equipment downstream (compressors).

At the intake of the first stage compressor the pressure is 12 bar (175 psi), and the discharge pressure is 43 bar (630 psi). As a normal process of compression the gas heats up and needs to be cooled down prior dehydration.

Another scrubber is installed before the second stage compressor which takes the dry gas at 42 bar (605 psi) and discharges it at 143 bar.

Again the dry gas must go through a cooler and a scrubber before entering the third stage compressor. At this point the dry gas is splitted into two streams; Lift gas for Eldfisk 2/7A and Eldfisk 2/7B, the pressure for this process is around 143 bar. The second stream goes to the third stage compressor where the pressure is raised to 220 bar. The gas from this last stage is for gas injection in Eldfisk 2/7A. This stage normally does not inject any gas and the majority of the time therefore all the gas is re-circulated making this stage inefficient.

All the process previously described is shown in figure 1.2.

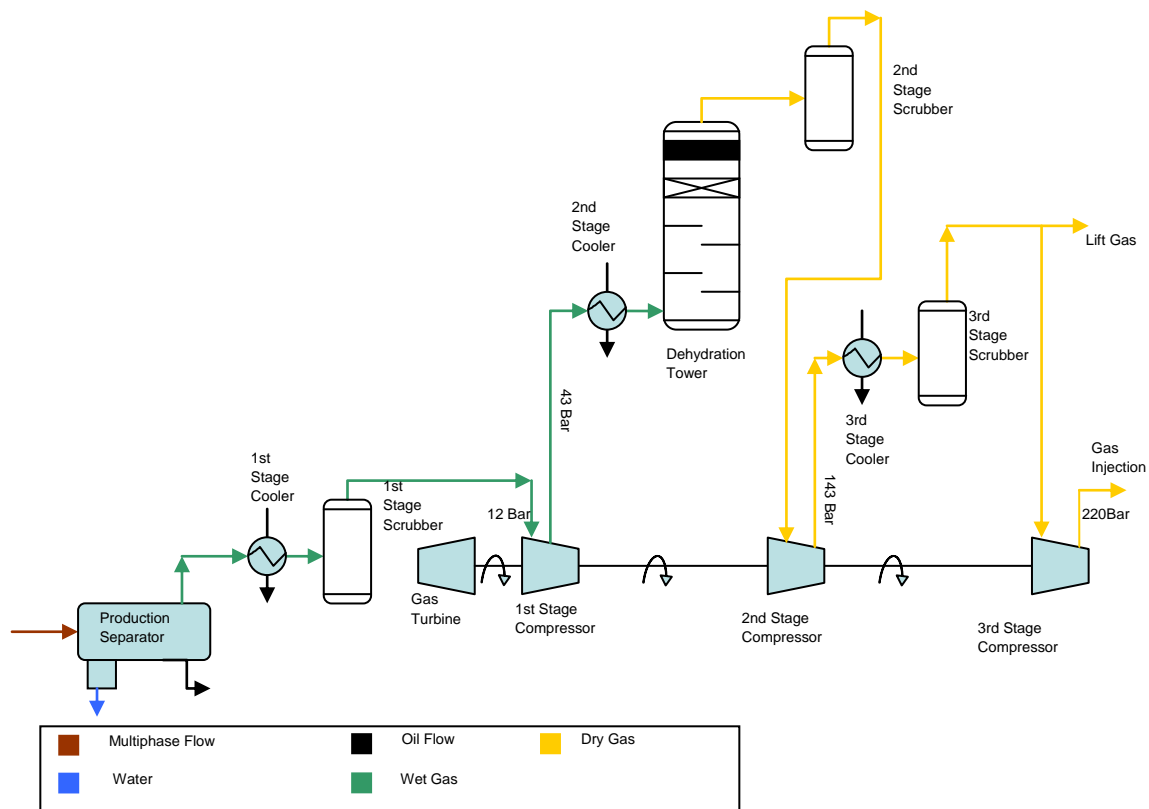


Figure 1.2: Simplified Process Flow Diagram of the Gas Compression System

## 1.2.Problem Statement

As time progresses, the water cut in the production line will increase due to water injection into the reservoir making more difficult the Gas Lift task.

The presence of large volumes of water in the production tubing will affect two important surface facility considerations.

- a) **Gas Lift Volume Rates** – Is the total lift gas requirement for the gas lifted wells. The requirement of lift gas will increase if the hydrostatic weight of the fluids is increased i.e. presence of water. Production will increase as a function of lift gas rates until a point of maximum production is reached (theoretical optimum), the addition of gas beyond this point will decrease productivity as a result of friction pressure loss dominance. Therefore a calculation of the new lift gas requirements due to the change in water cut is required.
- b) **Gas Lift Pressure** – Is a critical parameter in the gas lift system that has a major impact on the compression system design. One of the issues with the compression system results from the disparity between the discharge pressure for well kick-off, and

the required discharge pressure for continuous operation. The second issue is a result of the increasing water cut, where the discharge pressure will not be enough to move the fluid column efficiently until the discharge pressure of the compressor will be raised.

### 1.3.Objectives

“To optimize the lift gas compression system, as a result of the evaluation of gas lift volume rates and gas lift pressure.”

In order to “Optimize the Lift Gas Compression System”, the following sub-objectives will be taken into consideration:

- 1) To build a MatLab code able to estimate the theoretical optimum injection volume for the different gas lifted wells in Eldfisk field.
- 2) To determine new lift gas volume rates considering an augment in the water cut of the wells in eldfisk using the MatLab code.
- 3) To become acquainted with the lift gas injection pressure forecasted for the increasing water cut, and to estimate the discharge pressure from the compressor.
- 4) To Evaluate different scenarios that will allow achieving the estimated discharge pressure while taking into account the new volume for compression. This step will be done with a HYSYS simulation.

## Chapter 2. Methodology

For the sub-objectives declared in the previous chapter, the following table describes the methods used to achieve each one of it.

Table 2.1: Methodology

Design a Matlab Program	<ul style="list-style-type: none"> <li>• Construction of a Matlab code with a new approach for the calculation of the optimum lift gas injection rate</li> <li>• Use the Beggs and Brill (1973) method to create VLP curves</li> <li>• Use Vogel (1968) curves to create IPR curves</li> <li>• Use the minimum points of the different VLP curves and Cross-plot with the IPR to determine the production equilibrium (optimum) point.</li> <li>• For the estimated optimum, determine the oil production volume and gas rate of lift gas.</li> </ul>
Determine the volumes of gas needed for gas lift in Eldfisk wells	<ul style="list-style-type: none"> <li>• Gather well geometry data for each gas lifted well</li> <li>• Gather fluid characteristics data for each gas lifted well</li> <li>• Simulate in the MatLab code the wells</li> <li>• Create the gas lift performance curve for actual conditions and conditions where the water cut is increased,</li> <li>• Determine the economic optimum injection rate value for each gas lifted well in Eldfisk A and Eldfisk B</li> <li>• Sum up all the lift gas rates to know the total volume needed for compression in the theoretical optimum case, the economic optimum case and the increased water cut case</li> </ul>
To become acquainted with the lift gas injection pressure forecasted for the increasing water cut.	<ul style="list-style-type: none"> <li>• Gather information about which will be the lift gas injection pressure forecasted for the increasing water cut.</li> </ul>
Evaluate different scenarios to define the best way to achieve the discharge pressure	<ul style="list-style-type: none"> <li>• New gas rates and higher operating pressures could mean that the actual design and/or operating parameters should be modified.</li> <li>• Is the actual design enough to handle the new volumes and pressures, should it be modify?</li> <li>• Actual lift gas compression stage discharge pressure is 143 Bar, with the increasing water cut is thought to need 180 bar – 200 bar.</li> <li>• How can be achieved this pressure?             <ol style="list-style-type: none"> <li>1. Evaluate Different scenarios in a HYSYS simulation</li> </ol> </li> <li>• Determine which the best scenario is.</li> </ul>

## Chapter 3. Gas Lift Theory

### 3.1. Introduction

Oil producing wells will flow naturally for some period of time after they begin producing. Two main energy sources allow oil to flow until surface: Reservoir pressure and formation gas. As the well produces, these energy sources are consumed and at some point there is no longer enough energy available to flow naturally and the well will cease to flow. When the reservoir energy is too low for the well to flow, or the production rate desired is greater than the reservoir energy can deliver, it becomes necessary to put the well on some form of artificial lift to provide the energy to bring the fluid to the surface. (Schlumberger, 2000)<sup>(3)</sup>

The practice is that compressed gas is injected into the lower section of production tubing through a casing–tubing annulus and an orifice installed in the tubing string. Upon entering the tubing, (Brown, 1980)<sup>(4)</sup> describes that the compressed gas affects the liquid flow in two ways: (a) the energy of expansion propels (pushes) the oil to the surface and (b) the gas aerates the oil reducing the flowing bottom-hole pressure as a result of the reduced fluid density. To accomplish this efficiently, it is desirable to design a system that permits injection through a single valve at the greatest depth possible with the available injection pressure.

Gas lift technology has been widely used in the oil fields that produce sandy and gassy oils. Deviated holes present no problem. Well depth is not a limitation. It is also applicable to offshore operations. Lifting costs for a large number of wells are generally very low. However, it requires lift gas within or near the oil fields. It is usually not efficient in lifting small fields with a small number of wells if gas compression equipment is required. Gas lift advancements in pressure control and automation systems have enabled the optimization of individual wells and gas lift systems. (Guo et al, 2007)<sup>(5)</sup>

### 3.2. Gas Lift System

As stated before Gas Lift is the method of artificial lift which utilizes an external source of high pressure gas to be added to the production tubing with the objective to reduce the bottom-hole pressure and lift the well fluids. The availability of gas, compression systems and the cost of compression should be among the considerations to decide whether or not usage of Gas Lift as artificial recovery method is applicable. (Forero et al, 1993)<sup>(6)</sup>

A complete gas lift system consists of a gas compression station, a gas injection manifold with injection chokes and time cycle surface controllers, a tubing string with installations of unloading valves and operating valve, and a down-hole chamber. (Schlumberger, 2000)<sup>(3)</sup>

Figure 3.1 shows a configuration of a gas-lifted well with installations of unloading valves and operating valve on the tubing string. There are four principal advantages to be gained by the use of multiple valves in a well (Guo et al, 2007)<sup>(5)</sup>:

1. Deeper gas injection depths can be achieved by using valves for wells with fixed surface injection pressures.
2. Variation in the well's productivity can be obtained by selectively injecting gas valves set at depths "higher" or "lower" in the tubing string.
3. Gas volumes injected into the well can be "metered" into the well by the valves.
4. Intermittent gas injection at progressively deeper set valves can be carried out to "kick off" a well to either continuous or intermittent flow.

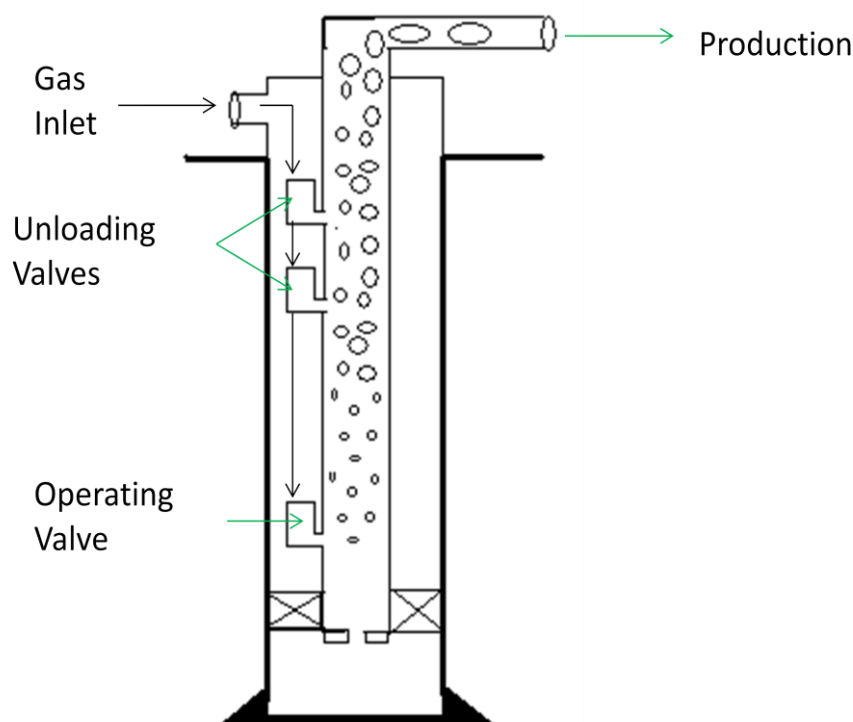


Figure 3.1: Configuration of a typical gas lift well. (Guo et al, 2007)<sup>(5)</sup>

A continuous gas lift operation is a steady-state flow of the aerated fluid from the bottom (or near bottom) of the well to the surface. Intermittent gas lift operation is characterized by a start-and-stop flow from the bottom (or near bottom) of the well to the surface.

In continuous gas lift, a small volume of high-pressure gas is introduced into the tubing to aerate or lighten the fluid column (Brown, 1980)<sup>(4)</sup>. This allows the flowing bottom-hole pressure with the aid of the expanding injection gas to deliver liquid to the surface. To accomplish this efficiently, it is desirable to design a system that will permit injection through a single valve at the greatest depth possible with the available injection pressure. (Schlumberger, 2000)<sup>(3)</sup>



The type of gas lift operation used, continuous or intermittent, is also governed by the volume of fluids to be produced, the available lift gas as to both volume and pressure, and the well reservoir's conditions such as the case when the high instantaneous BHP drawdown encountered with intermittent flow would cause excessive sand production, or coning, and/or gas into the wellbore. (Guo et al, 2007)<sup>(5)</sup>

The potential of gas lift wells is controlled by gas injection rate or gas liquid ratio (GLR). Four gas injection rates are significant in the operation of gas lift installations (Guo et al, 2007)<sup>(5)</sup>:

1. Injection rates of gas resulting in no liquid (oil or water) flow up the tubing. The gas amount is insufficient to lift the liquid. If the gas enters the tubing at an extremely low rate, it will rise to the surface in small semi-spheres (bubble flow).
2. Injection rates of maximum efficiency where a minimum volume of gas is required to lift a given amount of liquid.
3. Injection rate for maximum liquid flow rate at the “optimum GLR.”
4. Injection rate of no liquid flow because of excessive gas injection. This occurs when the friction produced by the gas prevents liquid from entering the tubing.

In general optimum gas lift conditions are achieved when gas is injected at the bottom of the production tubing. In this way the entire vertical column is less dense which yields to the lowest possible flowing bottom hole pressure, and therefore allowing a maximum drawdown hence maximizing the production rate. (Schlumberger, 2000)<sup>(3)</sup>

By increasing the gas injection rate the hydrostatic weight of the fluid column decreases, but at the same time the friction component increases. After the optimum point the friction component becomes the dominant pressure loss mechanism reducing the liquid recovery capability. (Economides, 1994)<sup>(7)</sup>

The increase in friction and the weight of the fluid column is proportional to the tubing length and its inclination; obviously in horizontal wells the benefits of continuous Gas Lift is limited to the vertical section of the well. (Brown, 1980)<sup>(4)</sup>

To determine the possible flow rates obtainable with Gas Lift is necessary to determine the Inflow Performance Relationship (IPR) of the well and compare it with the Vertical Lift Performance (VLP) of the production tubing when gas lifted to determine the operating point.

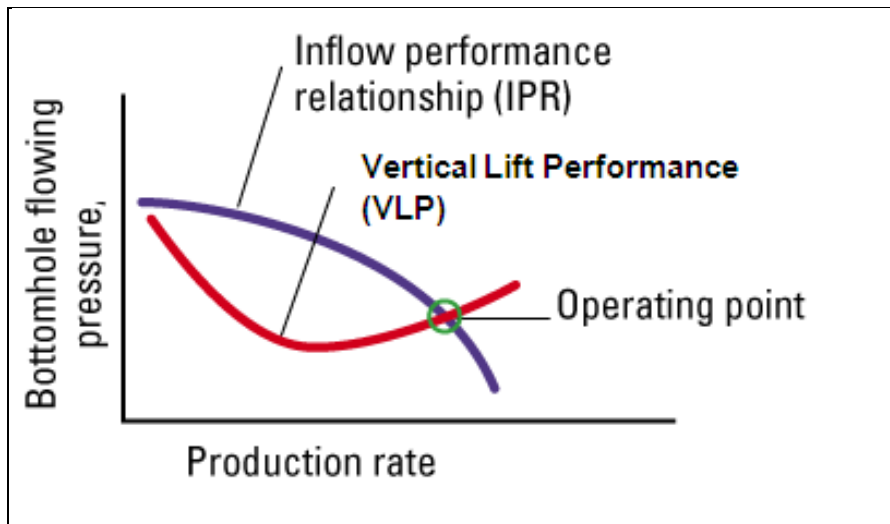


Figure 3.2: VLP & IPR curves (Economides, 1994)<sup>(7)</sup>

### 3.3. Inflow Performance Relationship (IPR)

The inflow performance of a well represents its ability to deliver fluids (Economides, 1994)<sup>(7)</sup>; an accurate prediction of the behavior of the production rate will allow an efficient Gas Lift design.

The inflow performance of a well depends greatly on the type of reservoir, drive mechanism reservoir pressure, permeability, etc. When taking into account the type of drive mechanism three different types of curves can be observed. (Schlumberger, 2000)<sup>(3)</sup>

- Straight line for water drive reservoirs, and/or reservoirs with pressure above the bubble point,
- Straight line with a small curvature at the end for gas cap drive reservoirs and,
- A clear curved line for solution gas drive reservoirs and/or reservoirs with pressure below the bubble point.

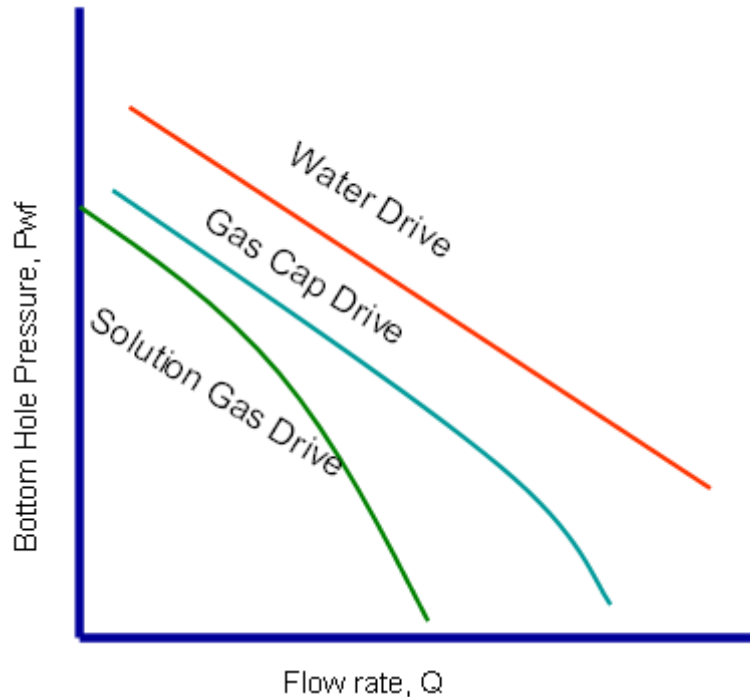


Figure 3.3: Typical Inflow Performance Curves (Schlumberger, 2000)<sup>(3)</sup>

It is also important to have in mind that the inflow performance behavior will not remain the same in time, but it will change with cumulative production and aging; therefore a continuous update of this parameter is crucial for artificial lift operations.

Since Gas Lift operations produce two-phase flow, and also the expansion of the gas is a driving mechanism for oil production, it is possible to compare this operation with the inflow performance associated to solution gas drive when the pressure is under the bubble point.

The solution of the curved inflow performance is challenging and yet they are not completely understood. In 1968 Vogel<sup>(8)</sup> proposed a solution to determine the inflow performance curve for solution gas drive for reservoirs below the bubble point.

Vogel developed an empirical solution that covers a wide range of oil PVT properties and relative permeability, at the same time to simplify the solution assumptions like circular, radial uniform flow with constant water saturation were made, also he neglected gravity segregation. (Vogel, 1968)<sup>(8)</sup>

Besides Vogel there are other models that can predict two-phase inflow performance relationships, like the work presented by Fetkovich (Fetkovich, 1973)<sup>(9)</sup> or Jones, Blount and Glaze (Jones et al, 1976)<sup>(10)</sup>; these are also empirical models and the accuracy of each model can change from well to well.

For this particular work Vogel dimensionless equation will be used in further calculations.

$$\frac{q_o}{q_{o,\max}} = 1 - 0.2 \left( \frac{P_{wf}}{P_r} \right) - 0.8 \left( \frac{P_{wf}}{P_r} \right)^2 \quad \text{Eq. 1}$$

### 3.4. Vertical Lift Performance (VLP)

The Vertical Lift Performance describes how the flow rate that reaches the surface is affected by the pressure drop in the tubing (Economides, 1994)<sup>(7)</sup>. For multiphase flow the prediction of the pressure drop profile is influenced by the phase behavior and properties, flowing temperature, flow pattern and the mechanical losses. The most common way to analyze this performance starts with a fixed back pressure (determined by wellhead or separator pressure) and according to the pressure losses the flowing bottom-hole pressure can be calculated

Predicting the pressure drop requires knowledge of flow formulas, based on the general momentum balance equation the total pressure gradient is made up of three different components. (Beggs, 1984)<sup>(11)</sup>

- Pressure Gradient due to elevation or potential energy change
- Pressure gradient due to frictional losses
- Pressure gradient due to acceleration or kinetic energy change

$$\frac{dP}{dL} = g\rho \sin \theta + \frac{fu^2 \rho}{2 \cdot D_{tubi}} + \rho u \frac{du}{dL} \quad \text{Eq. 2}$$

Since the mixture contains compressible fluids, the density of the mixture will depend on pressure and temperature variations and at the same time the velocity of the fluid will depend on the expansion of the fluid, therefore the solution of Eq. 2 or any other equation that allows to calculate the pressure drop will depend on an iterative process where the properties should be calculated at the average conditions of pressure and temperature. (Guo et al, 2007)<sup>(5)</sup>

As the properties should also be calculated at average temperature, the temperature profile inside the pipe can be calculated by means of the energy balance equation which depends on three terms (Hasan and Kabir, 2002)<sup>(12)</sup> having negative sign of Q, since the fluid is considered here to be the source of the heat to formation.

- Heat exchange by convection
- Change in kinetic energy
- Change of potential energy

$$(h_{z1} - h_{z2}) + \frac{(u_{z1}^2 - u_{z2}^2)}{2} - g\rho \sin \theta = -\frac{Q}{\dot{m}} \quad \text{Eq. 3}$$

Temperature and pressure profiles are important to predict the fluid behavior, i.e. phase change and development of new equilibrium among the different phases. Several works have been reported in literature. Some of the work involves approaches for temperature prediction for specific operation such as wellbore heat transmission Ramey jr. (1972)<sup>(13)</sup>; Chiu et al (1991)<sup>(14)</sup>, present a semi-analytical model to account for heat loss in deviated or horizontal wells, Alves et al (1992)<sup>(15)</sup> presented an approach for predicting temperature distribution in wellbores and pipelines, Hasan et al (1994)<sup>(12)</sup>, predicted heat transfer in two phase flow in wellbore and Romero(2005)<sup>(16)</sup> presented an approach for temperature profile in multilateral wells. Recently, Moradi et al (2011)<sup>(17)</sup> demonstrated the effect of temperature profiles in deep gas wells on the pressure.

Calculating the pressure of a mixture of fluids at any given point is a difficult task, and only with a complete understanding of multiphase flow a Gas Lift system can be designed efficiently.

Multiphase flow has been studied however not fully comprehended; consequently empirical correlations and mechanistic models were developed, the most accepted in the industry are: (Maurer Engineering, 1994)<sup>(18)</sup>

- Duns and Ros (1963)
- Hagedorn and Brown (1967)
- Aziz, Govier and Fogarasi (1972)
- Beggs and Brill (1973)

For this study the empirical model developed by Beggs and Brill was selected for the multiphase flow pressure drop calculations.

### 3.5. Beggs and Brill Model

The Beggs and Brill method works for horizontal, vertical flow or inclined flow. This method uses the general mechanical energy balance and the average in-situ density to calculate the pressure gradient. (Beggs & Brill, 1973)<sup>(19)</sup>

The Beggs and Brill (1973)<sup>(19)</sup> model was developed on the basis of experiments in small scale laboratory loops at the University of Tulsa. The test sections consisted of 90 feet long acrylic pipes with 1-1.5 inch inner diameter. The pipes could be arranged with arbitrary inclination.

Independent studies by Espanol et al (1969)<sup>(20)</sup>, Gregory et al (1980)<sup>(21)</sup>, found that the Beggs and Brill model is one of the most consistent empirical correlations to predict the pressure drop in vertical and inclined multiphase flow systems.

The prediction of flow patterns is the first step in any kind of model whether it is mechanistic or empirical. After determining the flow pattern, the liquid hold up is a key parameter to estimate the pressure drop in the tubing.

Beggs and Brill proposed 4 main kinds of flow patterns, which are segregated, intermittent, distributed and transition. Transition flow is the pattern where segregated flow is changing to intermittent or vice versa.

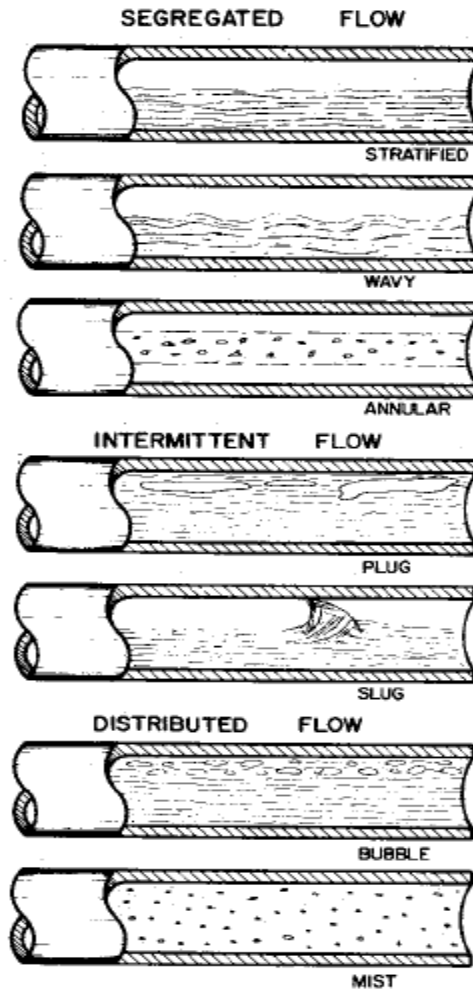


Figure 3.4: Flow Regimes Identified by Beggs and Brill (1973)<sup>(19)</sup>

The empirical method developed by Beggs and Brills is made of a set of equations (4 to 35) which allow the calculation of the pressure drop of a multiphase system, taking into account pressure losses due to friction, elevation and acceleration.

Superficial Velocity of the liquid Phase:

$$u_{sl} = \frac{q_l}{Area} \quad \text{Eq. 4}$$

Superficial Velocity of the gas Phase:

$$u_{sg} = \frac{\dot{m}_g}{\rho_g \cdot Area} \quad \text{Eq. 5}$$

Velocity of the Mixture

$$u_m = u_{sl} + u_{sg} \quad \text{Eq. 6}$$

Liquid Velocity Number

$$N_{lv} = u_{sl} \left( \frac{\rho_l}{g\sigma} \right)^{0.25} \quad \text{Eq. 7}$$

Froude Number

$$N_{FR} = \frac{u_m^2}{gD} \quad \text{Eq. 8}$$

No-slip liquid fraction

$$\lambda_l = \frac{u_l}{u_m} \quad \text{Eq. 9}$$

No-slip mixture density

$$\rho_{mns} = \rho_l \lambda_l + \rho_g (1 - \lambda_l) \quad \text{Eq. 10}$$

No-slip mixture viscosity

$$\mu_{mns} = \mu_l \lambda_l + \mu_g (1 - \lambda_l) \quad \text{Eq. 11}$$

Reynolds Number

$$Re = \frac{\rho_{mns} \cdot u_m \cdot D}{\mu_{mns}} \quad \text{Eq. 12}$$

L1, L2, L3 and L4 are correlation Boundaries

$$L_1 = 316\lambda_l^{0.302} \quad \text{Eq. 13}$$

$$L_2 = 0.0009252\lambda_l^{-2.4684} \quad \text{Eq. 14}$$

$$L_3 = 0.10\lambda_l^{-1.4516} \quad \text{Eq. 15}$$

$$L_4 = 0.5\lambda_l^{-6.738} \quad \text{Eq. 16}$$

### Determining flow regimes

Segregated if:

$$(\lambda_l < 0.01 \text{ and } N_{FR} < L_1) \text{ or } (\lambda_l \geq 0.01 \text{ and } N_{FR} < L_2)$$

Transition if:

$$(\lambda_l \geq 0.01) \text{ and } (L_2 < N_{FR} \leq L_3)$$

Intermittent if:

$$(0.01 \leq \lambda_l < 0.4 \text{ and } L_3 < N_{FR} \leq L_1) \text{ or } (\lambda_l \geq 0.4 \text{ and } L_3 < N_{FR} \leq L_4)$$

Distributed if:

$$(\lambda_l < 0.4 \text{ and } N_{FR} \geq L_1) \text{ or } (\lambda_l \geq 0.4 \text{ and } N_{FR} > L_4)$$

The following equation applies for segregated, intermittent and distributed flow regimes:

Horizontal Hold-up

$$Y_{10} = \frac{a\lambda_l^b}{N_{FR}^c} \quad \text{Eq. 17}$$

Hold-up at angle  $\theta$

$$Y_l = Y_{10}\psi \quad \text{Eq. 18}$$

With the constraint:  $y_{10} \geq \lambda_l$

$$C = (1 - \lambda_l) \ln(d\lambda_l^e N_{lv}^f N_{FR}^g) \quad \text{Eq. 19}$$

$$\psi = 1 + C[\sin(1.8\theta) - 0.333\sin^3(1.8\theta)] \quad \text{Eq. 20}$$

Where a, b, c, d, e, f and g depend on flow regimes and are given in the following table.



Table 3.1: Beggs and Brill Holdup constants

Flow Regime	a	b	c	
Segregated	0.98	0.4846	0.0868	
Intermittent	0.845	0.5351	0.0173	
Distributed	1.065	0.5824	0.0609	
Flow Regime and Direction	d	e	f	g
Segregated uphill	0.011	-3.768	3.539	-1.614
Intermittent downhill	2.96	0.305	-0.4473	0.0978
Distributed uphill	No correction, C=0 and $\psi=1$			
All regimes downhill	4.7	-0.3692	0.1244	0.5056

For transition flow, the liquid holdup is calculated as a weighted average of the segregated and the intermittent equations.

$$Y_l = A \cdot Y_l(\text{segregated}) + B \cdot Y_l(\text{Intermittent}) \quad \text{Eq. 21}$$

$$A = \frac{L_3 - N_{FR}}{L_3 - L_2} \quad \text{Eq. 22}$$

$$B = 1 - A \quad \text{Eq. 23}$$

The no slip friction factor  $f_n$  is based on smooth pipe ( $\varepsilon/D=0$ ) and the Reynolds number for no slip conditions.

$$f_n = \left( 2 \log \frac{\text{Re}}{4.2523 \log(\text{Re}) - 3.8215} \right)^{-2} \quad \text{Eq. 24}$$

$$y = \frac{\lambda_l}{Y_l^2} \quad \text{Eq. 25}$$

$$S = \frac{\ln(y)}{-0.0523 + 3.182 \ln(y) - 0.8725 [\ln(y)]^2 + 0.01852 [\ln(y)]^4} \quad \text{Eq. 26}$$

For the interval  $1 < y < 1.2$ , S is unbounded, therefore the equation becomes:

$$S = \ln(2.2y - 1.2) \quad \text{Eq. 27}$$

Now the two phase friction factor can be calculated from the following expression.

$$f_{tp} = f_n e^S \quad \text{Eq. 28}$$

The different pressure gradient now can be calculated.

Two phase mixture density

$$\rho_{tp} = \rho_l Y_l + \rho_g (1 - Y_l) \quad \text{Eq. 29}$$

Frictional Pressure Drop

$$\left( \frac{dp}{dz} \right)_f = \frac{f_{tp} \rho_{mns} u_f^2}{2D} \quad \text{Eq. 30}$$

Pressure drop due to elevation

$$\left( \frac{dp}{dz} \right)_{el} = g \rho_{tp} \sin(\theta) \quad \text{Eq. 31}$$

Acceleration pressure drop

$$\left( \frac{dp}{dz} \right)_{ac} = E_k \left( \frac{dp}{dz} \right) \quad \text{Eq. 32}$$

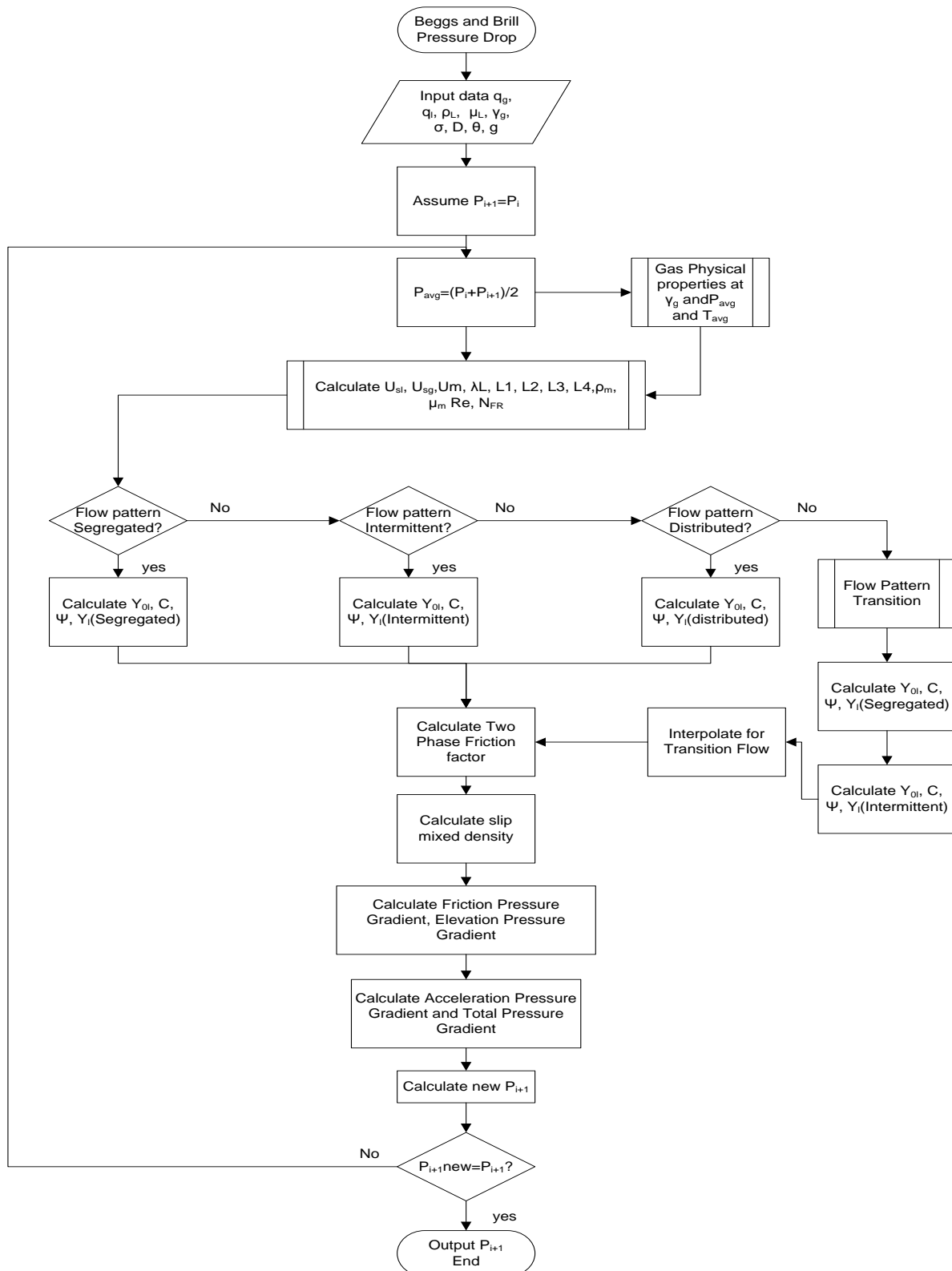
$$E_k = \frac{\rho_{tp} u_f u_{sg}}{P} \quad \text{Eq. 33}$$

$$\left( \frac{dp}{dz} \right) = \frac{\left( \frac{dp}{dz} \right)_f + \left( \frac{dp}{dz} \right)_{el}}{1 - E_k} \quad \text{Eq. 34}$$

Total Pressure drop

$$\left( \frac{dp}{dz} \right)_{Tot} = \left( \frac{dp}{dz} \right)_f + \left( \frac{dp}{dz} \right)_{el} + \left( \frac{dp}{dz} \right)_{ac} \quad \text{Eq. 35}$$

Figure 3.5 shows a flow diagram of the solution of Beggs and Brill Model.

Figure 3.5: Beggs and Brill Process flow Diagram (Beggs, 2002)<sup>(22)</sup>

### 3.6. Review of Gas Properties and Equation of State (EOS)

In every multiphase flow conditions gas is present, and in vertical flow this contributes to decrease the pressure gradient because its low density compared to liquids, although this decrease in pressure gradient has a limit; when there is excessive gas, the friction forces become dominant and the pressure drop increases. For horizontal flow the frictional forces are dominant at every moment increasing the pressure drop. (Beggs, 1984)<sup>(11)</sup>

It is of vital importance to know that in multiphase flow the properties of the fluids will change with pressure and temperature, but more significantly the properties of the gas will be affected, for that reason the success in the calculation of the pressure drop profile will depend on the accuracy of the properties of the injected gas (Barrufet et al, 1995)<sup>(23)</sup>. The properties that should be calculated carefully are the viscosity and the density and also its superficial velocity since it will change with the expansion of the fluid.

Three types of problems related to gases are involved when solving gas lift problems:

- Calculation of gas density at given pressure and temperature.
- Determination of the actual or real volume that a gas will occupy at the given pressure and temperature.
- The velocity of the gas in the pipe at the given pressure and temperature.

In order to understand and solve these problems a brief review of the Equation of State is given.

The real gas law is defined by the Eq. 36, where  $z$  is the compressibility factor and is the consequence of the ratio between the real volume and the ideal volume of the gas at given conditions of pressure and temperature.

$$PV = znRT \quad \text{Eq. 36}$$

Using the non-dimensional form of this EOS developed by Peng-Robinson (1975)<sup>(24)</sup> the deviation or compressibility factor was calculated and consequently other properties that depend on this parameter.

Non-dimension cubic Equation of State:

$$Z^3 - (1 - B)Z^2 + (A - 2B - 3B^2)Z + (B^3 + B^2 - AB) = 0 \quad \text{Eq. 37}$$

Temperature dependant dimensionless constant

$$A = \frac{P_f \cdot a(T)}{(R \cdot T_f)^2} \quad \text{Eq. 38}$$

Dimensionless constant

$$B = \frac{P_f \cdot b}{(R \cdot T_f)} \quad \text{Eq. 39}$$

Van der Waals co volume

$$b = \frac{0.07780 \cdot R \cdot T_{pc}}{P_{pc}} \quad \text{Eq. 40}$$

Characteristic constant dependent on the accentric factor

$$m = 0.37646 + 1.54226 \cdot \omega - 0.26992 \cdot \omega^2 \quad \text{Eq. 41}$$

Temperature scaling factor

$$\alpha(T) = \left( 1 + m \cdot \left( 1 - \sqrt{\frac{T_f}{T_{pc}}} \right) \right)^2 \quad \text{Eq. 42}$$

Attraction parameter

$$a(T) = \frac{0.45724 \cdot (R \cdot T_{pc})^2}{P_{pc}} \alpha(T) \quad \text{Eq. 43}$$

To simplify the calculations, the pseudo-critical conditions were calculated from the empirical correlation for natural gases presented by Brown and Katz (1944), therefore is not a compositional model however it depends on the specific gravity of the gas ( $\gamma_g$ ).

Pseudo-critical temperature of a natural gas

$$T_{pc} = 168 + 325\gamma_g - 12.5\gamma_g^2 \quad \text{Eq. 44}$$

Pseudo-critical pressure of a natural gas

$$P_{pc} = 667 + 15\gamma_g - 37.5\gamma_g^2 \quad \text{Eq. 45}$$

The viscosity of the gas will increase with pressure and temperature, the pressure effect is the same as in liquids, but the temperature effect is opposite. For this work the viscosity of the gas was calculated by using Lee et al correlation (1970) <sup>(25)</sup>; this correlation depends on the real density of the gas.

Viscosity of the Gas: calculated at real density ( $\rho$ , g/cm<sup>3</sup>) K, X and Y

$$\mu = Ke^{X\rho^Y} \quad \text{Eq. 46}$$

Constant K: calculated at M (Molecular weight) and T absolute temperature (°R)

$$K = \frac{(9.4 + 0.02M)T^{1.5}}{209 + 19M + T} \quad \text{Eq. 47}$$

Constant K: calculated at M (Molecular weight) and T absolute temperature (°R)

$$X = 3.5 + \frac{986}{T} + 0.01M \quad \text{Eq. 48}$$

Constant Y: calculated at X

$$Y = 2.4 - 0.2X \quad \text{Eq. 49}$$

### 3.7. Gas Lift Performance Curve

As mentioned before, while the lift gas volume is increased it will reach a point where the reduction in hydrostatic losses will get to a limit and frictional forces will be the dominant effect in the production tubing. After this point the well will produce less fluid. (Economides, 1994)<sup>(7)</sup>

This effect can be proved by a simple Pressure vs. Production Rate plot when comparing the IPR curve with the VLP curve for different gas injection rates or injection GLR (IGLR).

The conventional approach is summarized in the following figures.

As can be observed that when increasing the gas lift rate, the VLP intersect with IPR curve moves to a lower position, hence increases the production. After a critical injection rate, the intercept of IPR and VLP curves moves upwards consequently reduces the production rate. (Economides, 1994)<sup>(7)</sup>

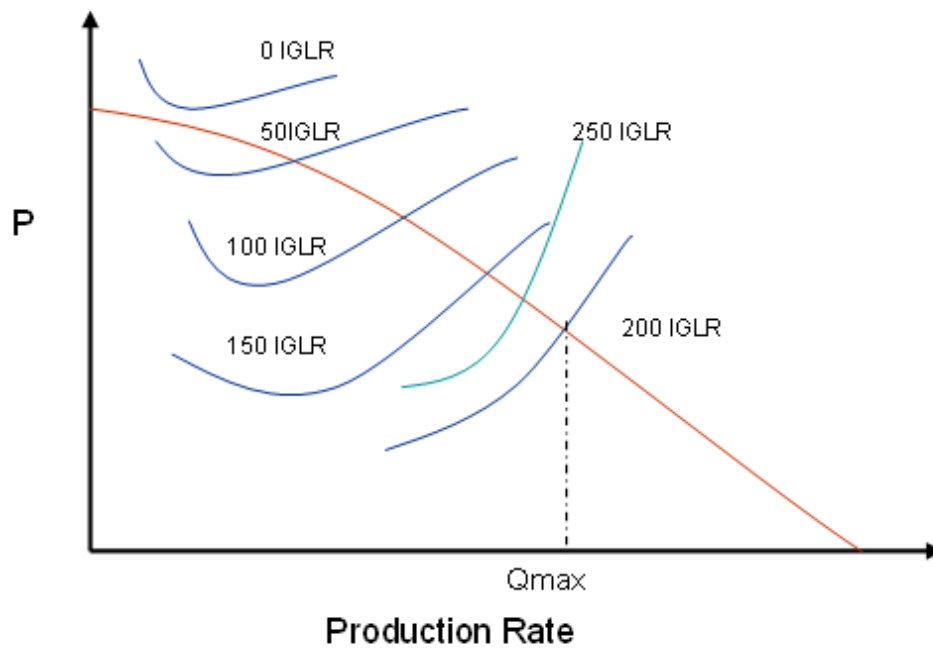


Figure 3.6: VLP curves for increasing gas injection rate

The second step of the conventional process is to plot the intercepts of the VLP and IPR curves, where the well production rate vs. lift gas injection rates produces a gas lift well performance curve as shown Figure 3.7.

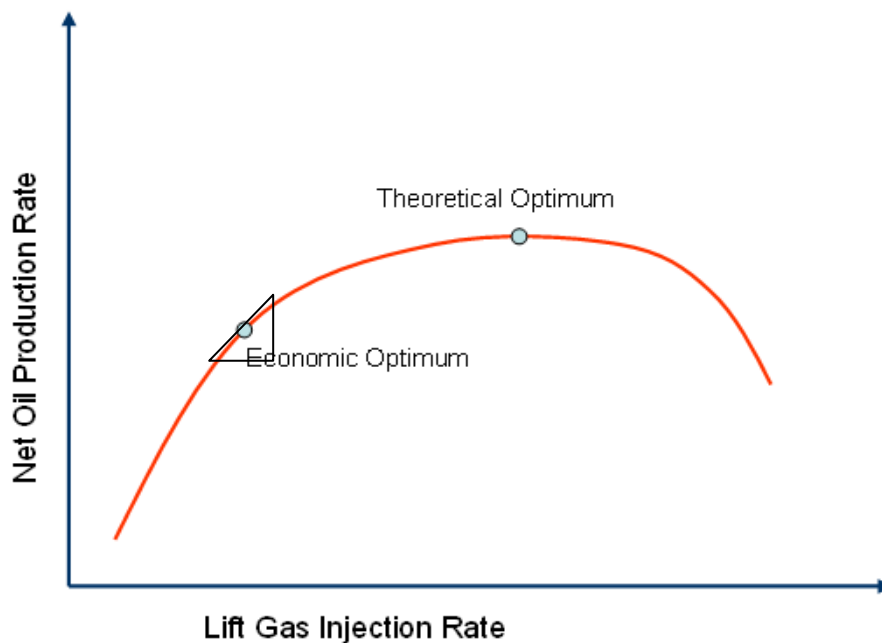


Figure 3.7: Gas Lift Performance Curve

The shape of this curve illustrates clearly the response of the well to the variation of lift gas volumes. This curve represents one of the most useful tools for gas lift design and also during operation. (Forero et al, 1993)<sup>(6)</sup>

It can be noticed that the slope of the gas lift performance curve decreases until it gets to zero at the maximum, therefore increments in gas injection will lead to increase the production rate, until the maximum is reached, after this point production will decrease. (Forero et al, 1993)<sup>(6)</sup>

The economic optimum will be lower than the theoretical optimum since it is located where a straight line with a slope equal to one is tangent to the Gas Lift performance curve, as it can be seen in figure 3.7.

The ability to predict correctly the performance of a Gas Lift well provides means of determining the amount of injection gas and the injection depth that will provide optimum gas lift operation for a given rate of fluid production. (A.F. Bertuzzi et al, 1953)<sup>(26)</sup>

The conventional approach that is presented above may miss the actual optimum gas injection rate due to the fact of that VLP curves may not coincide with the one that intersect with IPR curve that give the maximum rate. For this reason other methods that permit a direct calculation of the theoretical optimum are necessary; for example the optimum GLR can be found from traditional gradient curves such as those generated by Gilbert (Gilbert, 1954)<sup>(27)</sup>. The limitation of such curves is that they are numerous and applicable to certain conditions of tubing diameters and production rates; when the data is foreign to the available curves other methods must be applied.



## Chapter 4. Compression Theory

### 4.1 Introduction

A gas compressor is a mechanical device that increases the pressure of a gas by reducing its volume. (Halder, 2009)<sup>(28)</sup> Compressors are similar to pumps both increase the pressure on a fluid and both can transport the fluid through a pipe; the difference is because gases are compressible fluids and as a result, the compressor also reduces its volume.

The gas train consists of several stages; each stage takes the gas from a suitable pressure either from the production separator or from the gas outlet of the previous stage.

A typical stage is composed by a heat exchanger that cools down the gas, it then passes through a scrubber to remove all condensable liquids, and finally the gas goes to the compressor. (Devold, 2006)<sup>(29)</sup>

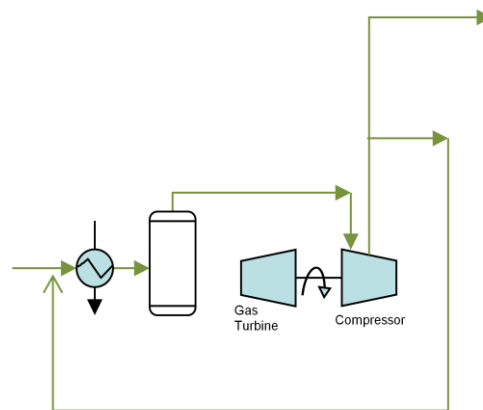


Figure 4.1: Typical Compression Stage

For Gas Lift operations the main issue with compressor selection normally results from the disparity between the discharge pressure for well kick-off, and that required for continuous operation at the deepest injection point. (Forero et al, 1993)<sup>(6)</sup>

The difference between kick-off pressure and operating pressure in many cases is so large that a single compressor cannot operate efficiently at both conditions. Attempts have been made in a number of projects to reconcile this problem by the provision of a separate, low volume, mobile high-pressure system for kick-off - with the main distribution system rated to the lower operating pressure. (Forero et al, 1993)<sup>(6)</sup>

### 4.2 Types of compressors

In the natural gas industry the reciprocating piston and centrifugal compressors dominate. Dominance by these two types occurs primarily due to their operating characteristics and

excellent fit to the pressure maintained in the pipe line system and the volumetric capacity requirements. (Murphy, 1989)<sup>(30)</sup>

In the reciprocating compressors a given quantity of air or gas is trapped in a compression chamber and the volume it occupies is mechanically reduced, causing a corresponding rise in pressure prior to discharge. At constant speed, the air flow remains essentially constant with variations in discharge pressure. (Bloch, 1996)<sup>(31)</sup>

Centrifugal compressors impart velocity energy to continuously flowing gas by means of impellers rotating at very high speeds. The velocity energy is changed into pressure energy both by the impellers and the discharge volutes or diffusers. In the centrifugal-type compressors, the shape of the impeller blades determines the relationship between flow and the pressure (or head) generated. (Aungier, 2000)<sup>(32)</sup>

An operating envelope for centrifugal and reciprocating compressors indicating capacity and pressure limitations is presented below in Figure 4.2.

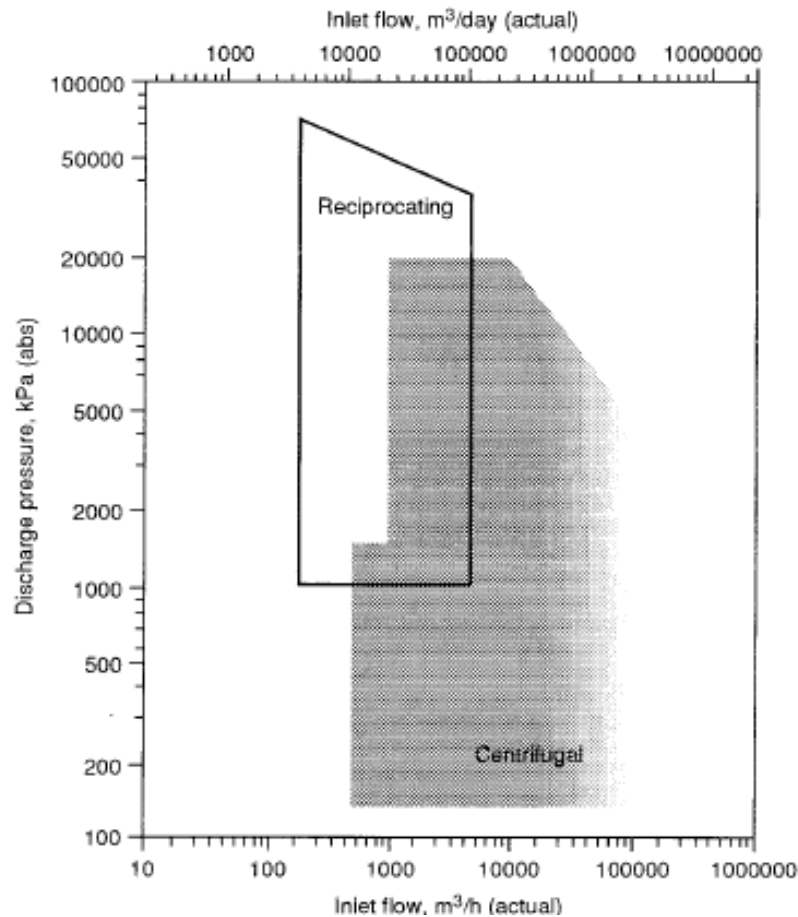


Figure 4.2: Operating envelope for centrifugal and reciprocating compressors (Forero et al, 1993)<sup>(6)</sup>

The selection of the compressors depends on many factors such as required discharge pressure, machine capacity and duty, operating environment, cost and available

space.(Forero, 1993) <sup>(6)</sup> Basic knowledge of selection criteria is considered essential although deep theory will not be discussed. Some of these criteria are compared in the following table.

Table 4.1: Comparison between the main types of compressors  
(Sustainable Development Office, 2002) <sup>(33)</sup>

Item	Reciprocating	Centrifugal
Efficiency at full load	High	High
Efficiency at part load	High due to Staging	Poor: below 60% of full load
Noise level	Noisy	Quiet
Size	Large	Compact
Vibration	High	Almost none
Maintenance	Many wearing parts	Sensitive to dust
Capacity	Low - High	Medium - High
Discharge Pressure	Up to 180 MPa	Up to 69 MPa

As it is clear from the comparative table the most appropriate type of compressors for offshore operation is the centrifugal type, since space is a real limitation over the platforms. In the view of the fact that the compressors operating on Edlfisk 2/7 E are from the centrifugal type, the following work will be based on this type of compressor.

### 4.3 Staged compression

Most compressors will not cover the full pressure range efficiently, whether the compressed gas is for pipeline, lift gas or reservoir reinjection. Therefore compression is divided into several stages to improve efficiency, maintenance and availability. (Devold, 2006) <sup>(29)</sup>

In the case of centrifugal compressors, commercial designs currently do not exceed a compression ratio of more than a 3.5 to 1 in any one stage (for a typical gas), usually limited by the discharge temperature mainly when compressing gases containing oxygen, which could support combustion, there is a possibility of fire and explosion because of the oil vapors present. (Perry, 2007) <sup>(34)</sup>

Since compression generates heat, the compressed gas is to be cooled between stages making the compression less adiabatic and more isothermal. The inter-stage coolers typically result in some partial condensation that is removed in vapor-liquid separators (scrubbers). (GPSA, 1998) <sup>(35)</sup>

Where multi-stage operation is involved, equal ratios of compression per stage are used (plus an allowance for pressure losses if necessary) unless otherwise required by process design. For two stages of compression the ratio per stage would approximately equal the square root of the total compression ratio; for three stages, the cube root. (GPSA, 1998) <sup>(35)</sup>

#### 4.4 Operating Parameters

The main operating parameters for a compressor are the actual volumetric flow and the discharge pressure, these two parameters will tell the operating RPMs of the compressor; it is important to mention that these parameters have some constraints given by the compressor design and performance. For example the maximum discharge pressure (Max Pd) or the maximum flow that the compressor can handle (Max Q). Also there is a minimum flow that the compressor can handle and this limit is set by the surge line (not enough gas to operate). (Devold, 2006) <sup>(29)</sup>

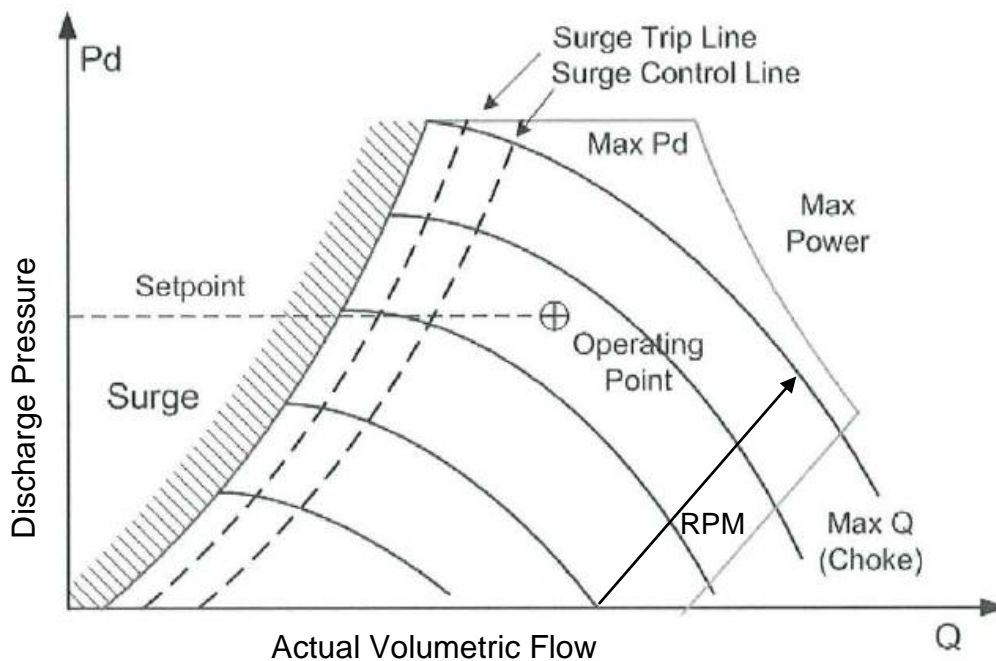


Figure 4.3: Typical Compressor Operating Curves. (Devold, 2006) <sup>(29)</sup>

#### 4.5 Anti-Surge Systems

The term “surge” indicates a phenomenon of instability which takes place at low flow values and which involves an entire system including not only the compressor, but also the group of components traversed by the fluid upstream and downstream of it. Surge is characterized by intense and rapid flow and pressure fluctuation throughout the system and is generally associated with stall involving one or more compressor stages. This phenomenon is generally accompanied by strong noise and violent vibrations which can severely damage the machines involved. (Hanlon, 2001) <sup>(36)</sup>

It is essential that all centrifugal compressor control systems be designed to avoid possible operation in surge which usually occurs below 50% to 70% of the rated flow. (GPSA, 1998) <sup>(35)</sup> The surge limit line (see Figure 4.3) can be reached from a stable operating point by either reducing flow or decreasing suction pressures.

The anti-surge control will protect the compressor from going into surge by operating the surge control valve. The basic idea of the anti-surge is that the system senses conditions approaching surge, and maintains the unit pressure ratio below the surge limit by recycling some flow to the compressor suction. Care must be taken to cool this recycle stream. (GPSA, 1998)<sup>(35)</sup>

Volume, pressure rise, or pressure ratio may be used as control parameters to sense an approaching surge condition. Such a condition will be established by the characteristic curve of the compressor.

As flow decreases to less than the minimum volume set-point, a signal will cause the surge control valve to open. The valve opens, as required, to keep a minimum volume flowing through the compressor. (Devold, 2006)<sup>(29)</sup>

#### 4.6 Prime Drivers

Centrifugal compressors can be driven by a wide variety of prime movers including electric motors, steam turbines, gas combustion turbines, and gas-expander turbines. Each driver has its own design parameters. (GPSA, 1998)<sup>(35)</sup>

A motor drive presents limitations in operation of the compressor due to constant and low speed. The constant speed restriction is minimized by suction or discharge throttling. The low speed restriction is corrected by introduction of a speed increasing gear. (GPSA, 1998)<sup>(35)</sup>

A steam turbine, on the other hand, has variable speed capability that allows more control of the compressor capacity or discharge pressure, and its high speed permits the compressor to be directly connected to the driver. In the case of a single-shaft gas turbine, the power output is limited at a reduced speed. (GPSA, 1998)<sup>(35)</sup>

The main type of drivers in the oil and gas industry and mainly over off-shore platforms are electrical motors and gas turbines.

**Gas Turbines** - The gas turbine was first widely used as an aircraft power plant. However, as they became more efficient and durable, they were adapted to the industrial marketplace. Over the years the gas turbine has evolved into two basic types for duty design and the aircraft derivative design. (GPSA, 1998)<sup>(35)</sup>

The industrial type gas turbine is designed exclusively for stationary use. Where high power output is required, 35000 hp and above, the heavy duty industrial gas turbine is normally specified. The industrial gas turbine has certain advantages which should be considered when determining application requirements. Some of these are: (GPSA, 1998)<sup>(35)</sup>

- Less frequent maintenance.
- Can burn a wider variety of fuels.
- Available in larger horsepower sizes.

**Electric Motors** – The electric motor drivers offer efficient operation and add flexibility to the design of petroleum refineries, petrochemical plants, and gas processing plants. Electric motors can be built with characteristics to match almost any type of load. They can be designed to operate reliably in outdoor locations where exposed to weather and atmospheric contaminants. (GPSA, 1998)<sup>(35)</sup>

Proper motor application is essential if reliable performance is to be achieved. Critical items to consider are load characteristics for both starting and operating conditions, load control requirements, power system voltage and capacity, and any conditions at the plant site that could affect the type of motor enclosure. (GPSA, 1998)<sup>(35)</sup>

## Chapter 5. Results and Discussions

As discussed in section 1.2 (Problem Statement) two of the major problems are related to Gas Lift Volume Rate and Gas Lift Pressure. This is the reason why this work was divided into two different parts. For the first part related to gas lift volume rate, a new approach was developed for the calculations of the optimum lift gas injection rate which yield maximum oil production.

With this new approach a MATLAB program was built to analyze the vertical lift performance of every well in the Eldfisk field that is under gas lift operations; since the problem of pressure drop in the tubing involves gas, oil and water flowing (multiphase flow), Beggs and Brill model (Beggs and Brill, 1973) <sup>(19)</sup> was selected for pressure drop calculations and the creation of the VLP curves.

Once defined the flowing conditions of every well the multiphase VLP curve was intersected with the Inflow Performance curve (IPR) developed by Vogel (Vogel, 1968) <sup>(8)</sup> due to its simplicity.

This analysis of the adequate gas lift volume rate was studied under two scenarios, the first one representing the actual conditions of the wells; and the second aiming to study the behavior when a change in water cut percentage will occur.

Once the requirements of gas are determined for actual conditions and increased water cut, there must be taken into considerations all the constraints that can set the limits of the optimizations of the compression system

Finally for the part related to Gas Lift pressure (compression), the volume resulting from the first part considering all the constraints was used as input data to perform the simulations in HYSYS; with the purpose of optimizing the compression system.

### 5.1. Gas Lift Volume

Estimating the maximum liquid production rate (theoretical optimum) by the conventional approach as it is shown in Figures 3.6 and 3.7 is not an easy task, since it may miss the actual optimum gas injection rate due to the fact of that VLP curves may not coincide with the one that intersect with IPR curve that give the maximum rate.

The approach suggested here is to overcome this problem. The approach starts by estimating the minimum bottom-hole flowing pressure for a different set of VLP curves. Production rates are usually associated with minimum bottom-hole pressure, where the draw down increases.

The obtained minima of the bottom-hole pressure ( $P_{wf}$ ) from various VLP curves, which are related to different gas lift injection rate as shown in fig. 5.1a, are plotted in fig. 5.1b with the

abscissa representing the liquid production rate and the vertical axis represents the bottom-hole pressure. The intersection between the IPR curve and the line representing the  $P_{wf}$  minima is the optimum/maximum production rate for the system. This is, then, related to gas lift injection rate from fig.5.1a, for convenience and clarity a new figure (fig.5.1c) is constructed. GLR represent the total GLR, i.e. natural and injected gas liquid ratio. The preference of using injection GLR is due to the fact pressure drop associated with gas injection would cause natural GLR to expand, which may enhance the lifting performance.

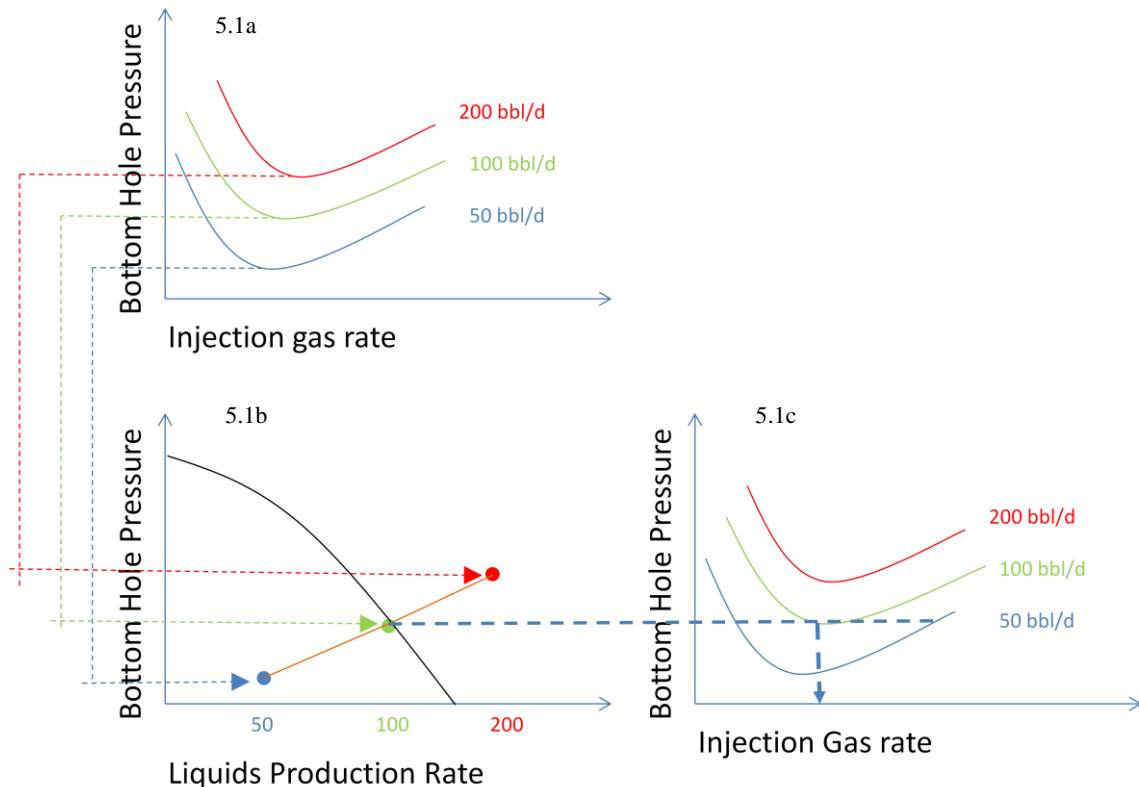


Figure 5.1: Method proposed to calculate the theoretical optimum

### 5.1.1 Optimum Gas Lift Injection Rate

With the method presented above all the gas lift wells from the Eldfisk field (13 wells from Eldfisk 2/7 A and 5 wells from 2/7 B) were simulated to estimate the optimum lift gas injection rate that is needed to produce the maximum amount of oil possible.

Since the results are mainly graphical outputs from the MATLAB code, the figures corresponding to well A-06 will be analyzed in the main body of this document. The figures belonging to the rest of the wells can be observed in appendix A.

In addition Table 5.1 shows a quantitative summary of the results obtained in every well.



## i. Well A-06

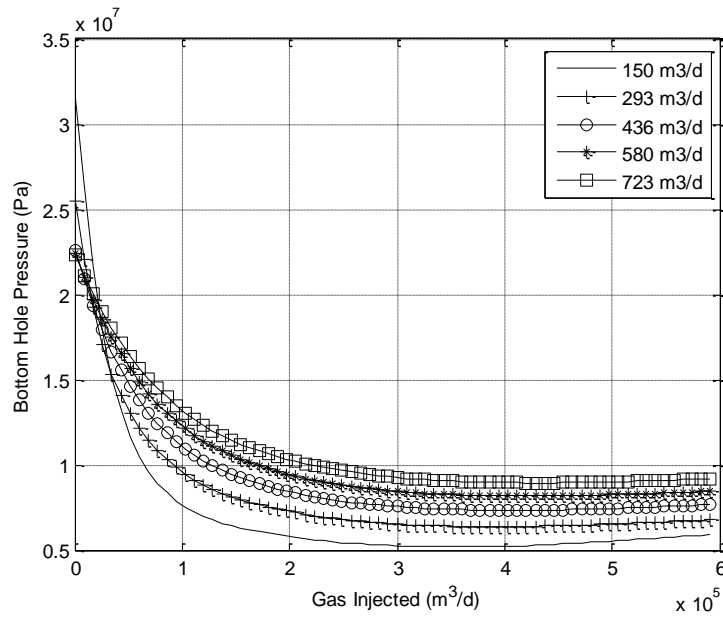


Figure 5.2: VLP curves for Well A-06

By taking the minimum values of each curve it is possible to create the maximum draw-down curve and to plot it against the IPR of the well to determine the maximum oil production rate.

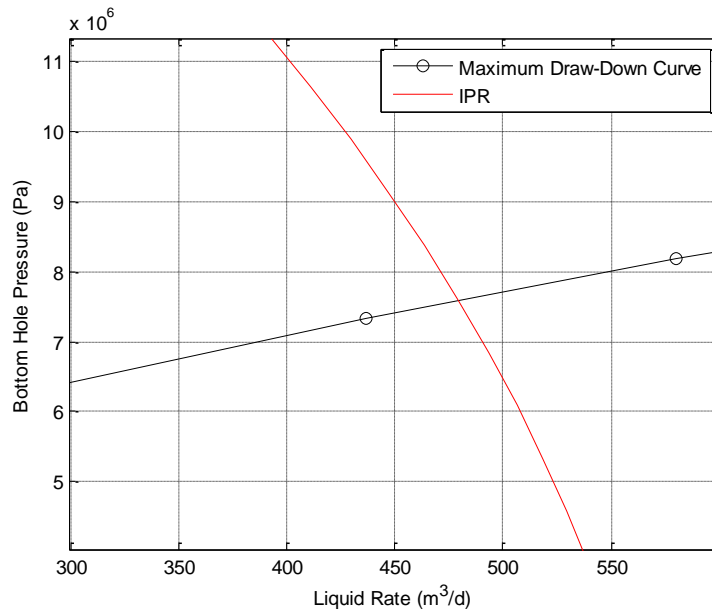


Figure 5.3: VLP vs. IPR for well A-06

Following the procedure in Figure 5.1 it is possible to determine that for well A-06 the optimum gas injection rate is  $407940 \text{ m}^3/\text{d}$ , allowing a maximum oil production rate of  $479 \text{ m}^3/\text{d}$ .

To summarize the results obtained in the simulations, the following table has been put together.

Table 5.1: Summary of the optimum injection and oil production values per well

Well	Optimum oil production m <sup>3</sup> /d	Optimum gas injection sm <sup>3</sup> /d
A1	284	188 470
A2	455	250 800
A3	180	207 500
A6	479	407 940
A10	80	151 145
A16	261	302 910
A17	395	200 190
A18	179	207 880
A19	324	295 740
A20	348	206 190
A23	385	206 980
A26	158	186 940
A28	436	409 070
B10	24	227 125
B11	145	172 560
B14	548	258 670
B17	592	344 050
B19	522	320 320
<b>TOTAL</b>	<b>5 793</b>	<b>4 544 480</b>

Assuming that an unlimited amount of gas is available to gas lift the wells in the Eldfisk field the maximum oil production that can be achieved is 5 793 m<sup>3</sup>/d (36 535 bbl/d). Eldfisk 2/7 A is the main contributor to the oil production but evidently at the same time needs larger volumes of lift gas.

To produce a maximum volume of 3 961 m<sup>3</sup>/d in Eldfisk 2/7 A; it is necessary to inject 3 221 755 sm<sup>3</sup>/d of gas. Simultaneously for Eldfisk 2/7 B to produce a maximum oil rate of 1832 m<sup>3</sup>/d needs 1 322 725 sm<sup>3</sup>/d.

The total demand of lift gas in the Eldfisk field sums up to 4 544 480 sm<sup>3</sup>/d; equivalent to 160.46 MMscfd.

Knowing that the actual volume of gas processed on Eldfisk 2/7 E is 52 MMscfd and that the gas lift valves in the different wells have an operating limit of 3.5 MMscfd; a different kind of approach must be done considering the restrictions previously mentioned; therefore the economic optimum for every well will be estimated by using the gas lift performance curve.

### 5.1.2 Economic Optimum Gas Lift Injection Rate

In this section, the gas lift performance curve is plotted to identify the economic optimum for the different wells. At the same time, in this section will be included the analysis of the Gas Lift performance curve when an increment in the water cut occurs.

The analysis for the increased water cut scenario assumes that the only variable which has changed is the water cut percentage. The rest of the variables were not modified since no further information was available.

The study of the gas injection rate for the increased water cut scenario will target to estimate the gas injection rate needed to keep the total oil production rate of the field equal to the actual production rate matching the economic optimum.

In this point is important to recall Figure 3.7 where it can be seen that the economic optimum will be lower than the theoretical optimum since it is located where a straight line with a slope equal to one is tangent to the Gas Lift performance curve.

Following this criteria the economic optimum of every well was calculated. Continuing with the study of well A-06 the following picture is depicted. The gas lift performance curve of the remaining wells can be found in Appendix B.

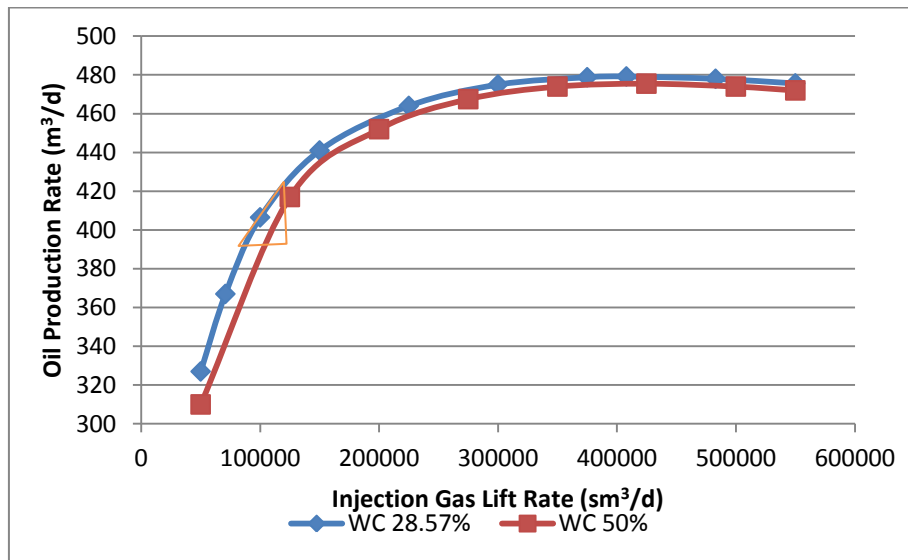


Figure 5.4: Gas Lift Performance Curve for Well A-06

The economic optimum for well A-06 is located at 100 000 sm<sup>3</sup>/d, which will allow to produce 406 m<sup>3</sup>/d. In the case of an increase in the water cut, the volume of gas needed to produce 16 m<sup>3</sup>/d of oil less considering the increase of water production will remain 100 000 sm<sup>3</sup>/d.

Well B-10 is a special well where the actual water cut is so high (94.29%) that a forecast for a scenario where the water cut will increase has not been performed, and instead directly assumed that the well will be shut down.

Although the economic optimum is more likely to be higher, for well B-10 in this opportunity will be assumed to be located at 50000  $\text{sm}^3/\text{d}$ , due to its low oil production rate, the increase of oil production is so small that is not a highly attractive well. With this lift gas volume the well will produce 18  $\text{m}^3/\text{d}$ .

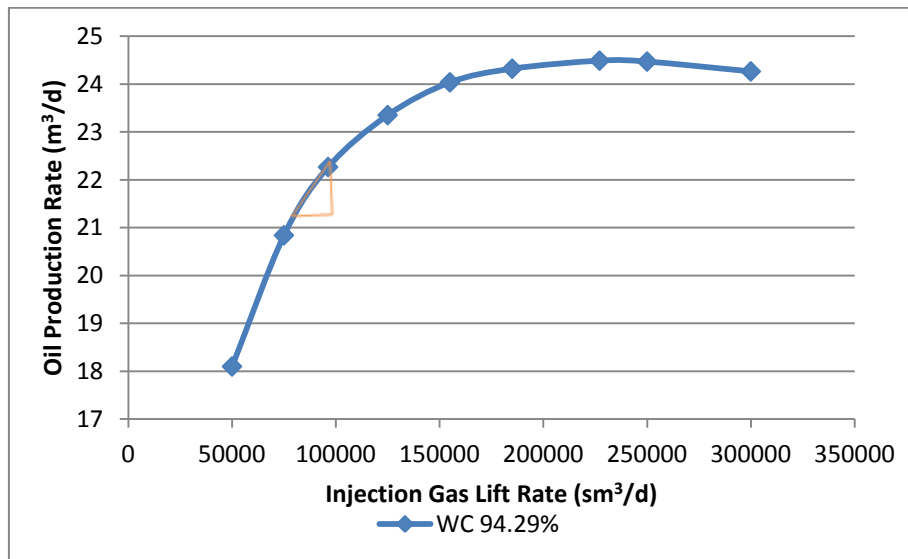


Figure 5.5: Gas Lift Performance Curve for Well B-10

Table 5.2 shows a quantitative summary of the results obtained in every well with the purpose to go over all the results obtained for the economic optimum gas volume to be injected for the actual conditions

Table 5.2: Summary of the economic optimum injection and oil production values per well

Well	Economical oil production m <sup>3</sup> /d	Economical gas injection sm <sup>3</sup> /d
A1	269	85 000
A2	356	50 000
A3	169	74 455
A6	406	100 000
A10	78	87 500
A16	237	85 400
A17	363	75 000
A18	160	50 000
A19	285	85 000
A20	327	85 000
A23	355	75 000
A26	153	85 000
A28	351	90 000
B10	18	50 000
B11	138	70 792
B14	471	75 000
B17	481	96 480
B19	450	97 896
<b>TOTAL</b>	<b>5 067</b>	<b>1 417 523</b>

Knowing that the amount of gas is available to gas lift the wells in the Eldfisk field is not enough for maximum oil production; the production that can be achieved when an economical approach is done is 5 067 m<sup>3</sup>/d (31 870 bbl/d).

For the economic optimum scenario the total demand of lift gas in the Eldfisk field is 1 417 523 sm<sup>3</sup>/d; equivalent to 50 MMscfd.

It is interesting to notice that the economical approach will lead to a reduction of 70% (110 413 MMscfd, more than twice the available volume) of the lift gas demand while the oil recovery will decrease only in 12%.

In figure 5.6 a comparison of the results obtained with the simulations performed and the actual measured oil production volumes can be observed.

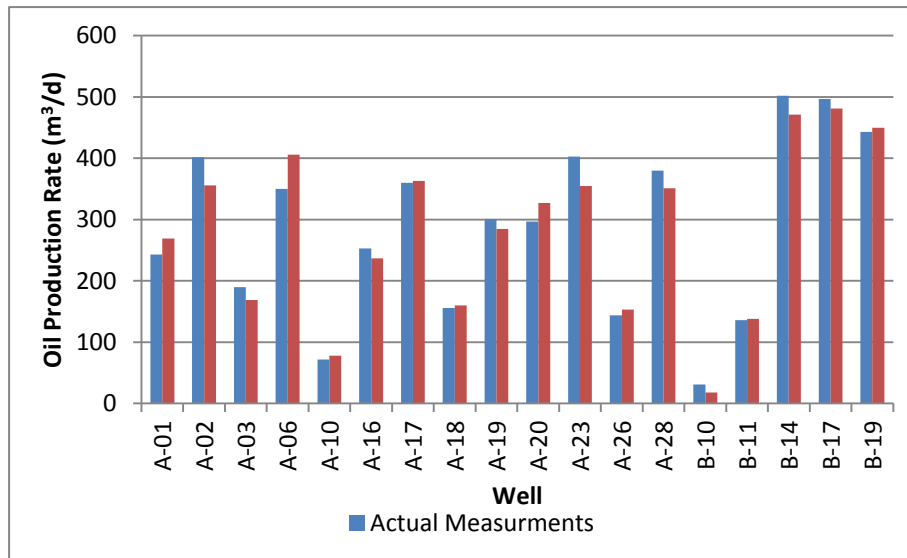


Figure 5.6: A comparison of the Results obtained and the actual measurements

Knowing that gas lift operations in the Eldfisk complex follow the economic optimum design, it is obvious that there exists a variation between the actual measurements and the results of the simulations performed in this work; this difference can be attributed to the use of empirical models such as Beggs and Brill (1973) for the pressure drop calculation, and the use of Vogel (1968) equation for determining the inflow performance of the wells.

Also the simulation code has two important simplifications; first it uses only one size of production tubing diameter, when in reality the diameter in the production tubing is not unique. The second simplification is related to the direction of the well. Rather than taking into account the real path of the well, the simulation code takes the wells as to be slanted, considering an angle of inclination calculated from the difference between Measured Depth (MD) and True Vertical Depth (TVD).

Finally to understand how an increment in the water cut percentage will affect the oil production system and the lift gas demand table 5-3 has been put together.

The objective of this analysis is to understand the effect of larger volumes of water in the fluid column inside the production tubing. If it is desired to maintain the oil production rates from the field without going beyond the economical boundary. How much more gas will be needed to lift the heavier column?

From Table 5.3, it can be observed that the total amount of lift gas for this scenario will be 1 616 851  $\text{sm}^3/\text{d}$  (57 MMscfd), 5 MMscfd more than the available volume, since this scenario is a consideration for the future, this negative difference can be balanced when Eldfisk 2/7 S will come on line since it is forecasted the total volume available will be 120 MMscfd with this platform that will substitute Eldfisk FTP.

Table 5.3: Summary of the economic optimum injection and oil production values per well for the increased water cut scenario

Well	economical oil production m <sup>3</sup> /d	economical gas injection sm <sup>3</sup> /d
A1	264	85 396
A2	383	75 000
A3	161	76 455
A6	390	100 000
A10	76	100 000
A16	238	100 000
A17	360	90 000
A18	160	65 000
A19	285	100 000
A20	321	95 000
A23	360	110 000
A26	151	95 000
A28	353	125 000
B11	137	80 000
B14	470	100 000
B17	476	110 000
B19	443	110 000
<b>TOTAL</b>	<b>5038</b>	<b>1 616 851</b>

## 5.2 Optimization of the compression train

The gas compression train is a three stage compression system as it is described in Chapter 1. Second stage was designed to have as intake the gas coming from the dehydration system and to discharge it for gas lift operations at approximately 143 bar. Third stage compression is designed for gas injection to the reservoir, although the majority of the time there is no injection therefore the gas is just re-circulating.

After this short description, for this work there have been detected three important problems.

- Insufficient Discharge pressure for gas lift operations.
  - Due to increasing water cut
  - Kick-off of the wells needs higher pressure than when operating
- High re-circulation in compression stages
  - Scrubbers working to limit capacity
- Third stage re-circulates almost all the gas, becoming a very inefficient stage.

Part of the optimization of the compression train is related to the insufficient discharge pressure due to the change in water cut. The goal is to increase the discharge pressure for gas lift operations from 143 bar to 180 - 200 bar. To achieve this target 5 scenarios are proposed for analysis.

- 1) Decreasing RPM (8872 RPM)
- 2) Decreasing RPM (8872 RPM)+Electric Motor in 3rd stage
- 3) Increasing RPM (9920 RPM)
- 4) Original Design+ Electric Motor in 3rd stage
- 5) Decreasing RPM (8560 RPM)

The idea of analyzing more scenarios where decreasing the RPMs could be a solution, resides in three benefits:

- The overall compression energy consumption will be decreased.
- The third compression stage will be used to deliver gas with higher pressures for gas lift wells.
- Decreasing the RPMs can allow a bigger margin for reducing the re-circulating gas in all the stages.



On the other hand increasing the RPMs of the compressors represents a fast and easy solution since all the design will not need any modification and the pressure requirements will be fulfilled without further complications although the power consumption will be increased.

Finally those scenarios that involve the usage of an electrical driver for the third stage of compression will allow a larger flexibility on the discharge pressures, flexibility that cannot be obtained with a single shaft compression train as it happens in the actual design. The disadvantage of these scenarios is that they require a modification in the system, which means investment and also more space to accommodate the new equipment.

Figure 5.7 explains the advantage of how a reduction in the speed of the compressor can allow a reduction in re-circulating gas flow. Point number 1 represents any actual operating point, by reducing the recycled flow the operating point can be taken to number 2 close to the surge control line and at the same time this movement allows increasing the discharge pressure, by reducing the speed of the compressor (point 3) the discharge pressure decreases but also it gives some more freedom to reduce the re-circulating flow until point number 4 is reached before the surge control line, also at this point it can be seen that the discharge pressure is just a bit lower than at the initial operating conditions in point 1.

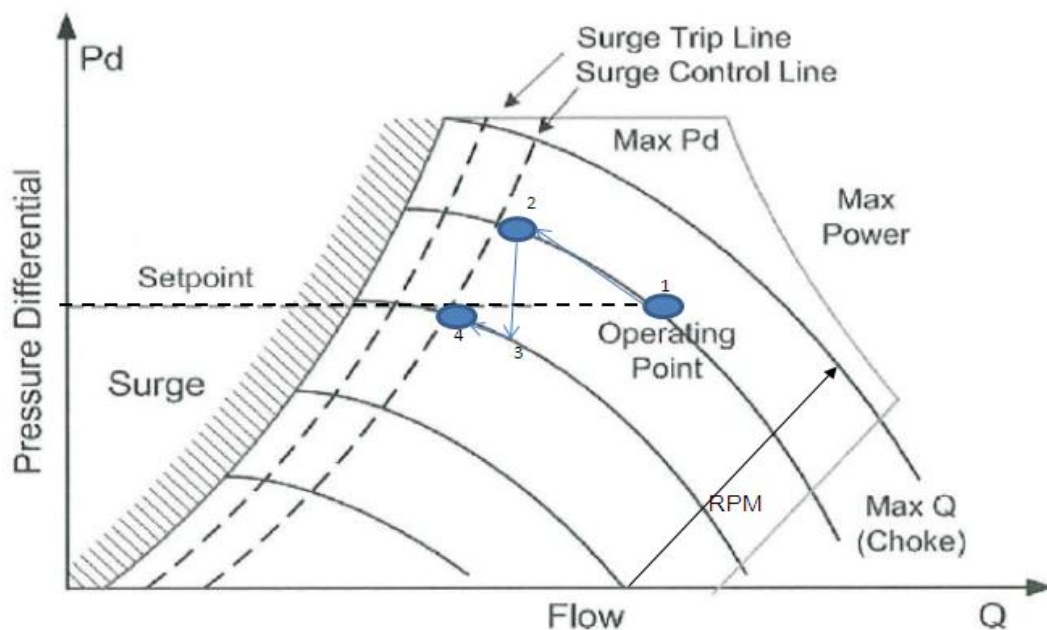


Figure 5.7: Modified Operating conditions in typical compression head curves

The head curves of the three compressors had been modeled in HYSYS to include a real analysis of the compression behavior of each stage in the compression system of Eldfisk 2/7 E.

The gas flow calculated in the previous section for the economic optimum design (50 MMscfd) and the five scenarios previously proposed are used as input information to calculate the power consumption and recirculation rates for the whole system and per stage.

The simulation of the different scenarios were carried out in a HYSYS simulation case; where all the equipment present in the real process flow diagram of the compression train on Eldfisk 2/7 E was included.

Also the tag numbers of the equipment in the HYSYS case are the same as those that correspond to the equipment in the real process.

For the scenarios previously proposed the power consumption and recirculation rates are shown in tables 5.4 to 5.6.

Table 5.4: Proposed Scenarios and Results for First Compression Stage

Option	Intake (bar)	Discharge (bar)	Compressor Power (kW)	Recirculation Kg/h
Actual Operating Design 9095 RPM	13	43.61	6 736	124 800
Decreasing RPM (8872 RPM)	13	40.98	6 332	119 300
Decreasing RPM (8872 RPM)+EM	13	40.98	6 332	119 300
Increasing RPM (9920 RPM)	13	47.95	7 364	131 200
Original Design+ Electric Motor 3 stg. (8900RPM)	13	43.61	6 736	124 800
Decreasing RPM (8560 RPM)	13	36.77	5 396	119 300

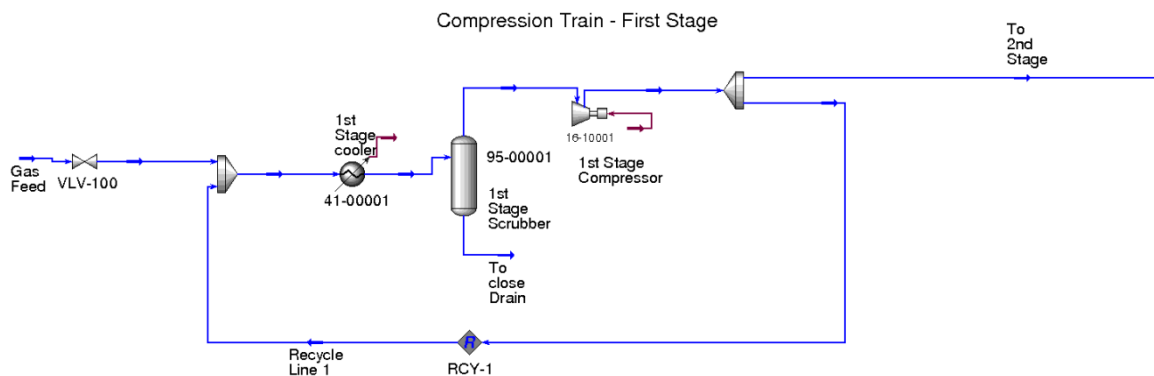


Figure 5.8: Compression Train – First Stage

In the first stage the compressor is re-circulating almost 125 000 Kg/h allowing a discharge pressure of approximately 44 bar. Since this compressor is already operating close to the surge line a large reduction in the re-circulating rates is not possible. To keep the compressor operating in the safe limits a maximum of 6% of the re-circulation can be reduced. As it was explained before the effect of increasing the speed of the compressor is raise in the discharge pressure and an increase of the re-circulating rates is necessary to keep the compressor away from going into surge.

Table 5.5: Proposed Scenarios and Results for second Compression Stage

Option	Intake (bar)	Discharge (bar)	Compressor Power (kW)	Recirculation Kg/h
Actual Operating Design 9095 RPM	42.61	143	5 591	110 000
Decreasing RPM (8872 RPM)	39.98	124	4 622	81 780
Decreasing RPM (8872 RPM)+EM	39.98	124	4 622	81 780
Increasing RPM (9920 RPM)	46.95	181	6 715	125 500
Original Design+ Electric Motor 3 stg. (8900RPM)	42.61	143	5 591	110 000
Decreasing RPM (8560 RPM)	36.77	101.9	3 675	71 260

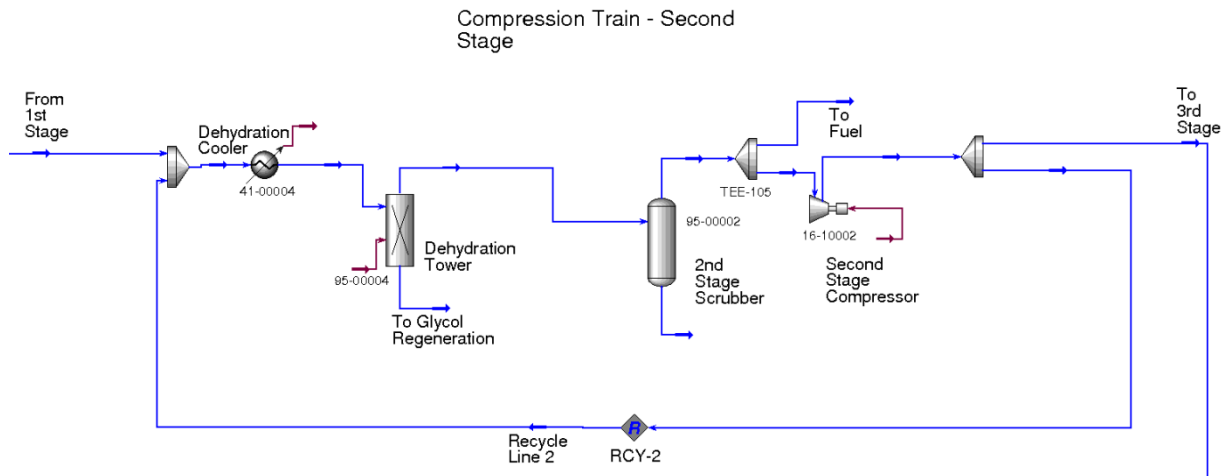


Figure 5.9: Compression Train – Second Stage

Second stage of compression is more interesting since it allows bigger modifications to the operating parameters related to the head curves. For example re-circulating rates can be reduced 25%-35% and the compressor power 17% - 34%. On the other hand if the speed of the compressor is increased it can be seen that the power of the compressor and the recirculation rates are also increased and as result a higher discharge pressure is obtained. This discharge pressure is between the limits specified for discharge pressure for the gas lift system (180 bar – 200 bar).

Table 5.6: Proposed Scenarios and Results for Third Compression Stage

Option	Intake (bar)	Discharge (bar)	Compressor Power (kW)	Recirculation Kg/h
Actual Operating Design 9095 RPM	138	220	2 743	155 700
Decreasing RPM (8872 RPM)	119	195	2 240	144 300
Decreasing RPM (8872 RPM)+EM	119	187.3	938	98 130
Increasing RPM (9920 RPM)	176	270	3 383	190 000
Original Design+ Electric Motor 3 stg. (8900RPM)	138	190	1 196	130 700
Decreasing RPM (8560 RPM)	96.9	181.2	763.7	71 260

The objective of the study of the final compression stage is to verify if the discharge pressure of the different scenarios where the speed of the compressor has been decreased will be enough to satisfy the demands of discharge pressure for gas lift operations (180 bar – 200 bar). As it can be observed from the Table 5.6 the discharge pressure will be between the established limits of 180 bar – 200 bar. One thing to highlight from this table is the usage of electric motors as drivers and how they can reduce the power consumption of the compressors (65% - 72%).

Since the minimum pressure for injection to the reservoir is 206 bar. The scenario where the speed of the compressor is reduced to 8872 RPM during reservoir injection periods will not sustain the pressure demands, and it will be necessary only during those periods to supply pressurized gas for injection by increasing the speed of the compressor.

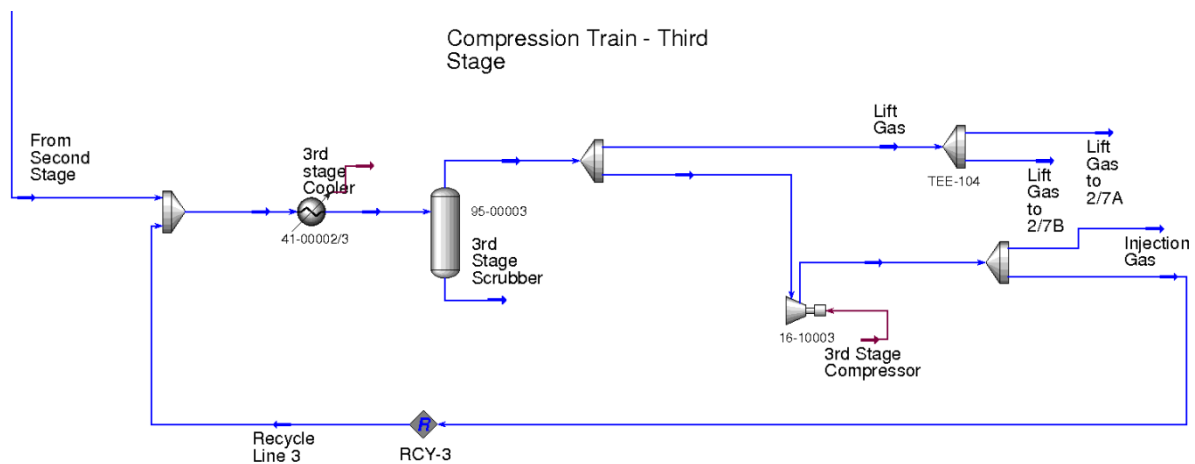


Figure 5.10: Compression Train – Third Stage

Using the scenario where the speed of the compressor is 8872 RPM together with an electric motor in the last stage can offer more flexibility if higher pressures are needed, but it must also be considered that the new equipment will occupy more space and will need investment to adequate the existing facilities.

Finally a comparison of the total power consumed by the compression train in the different scenarios can be observed in table 5.7.

Table 5.7: Comparison of the total power consumption

Total Power consumption	KW
Original Design 9095 RPM	15 070
Decreasing RPM (8872 RPM)	13 194
Decreasing RPM (8872 RPM)+EM	11 892
Increasing RPM (9920 RPM)	17 462
Original Design+ Electric Motor 3 stg. (8650RPM)	11 523
Decreasing RPM (8560 RPM)	9 834.7

Another parameter that must be considered is the waste heat recovery unit, this unit used for steam and electricity production, it recovers heat from the exhaust line of the turbine and if the power consumption is decreased significantly it can affect negatively the electricity production of the field.

Now that the entire advantages and disadvantages of all the scenarios were discussed, the scenario that fits best all the considerations seems to be scenario number one with the only disadvantage that during periods of injection to the reservoir, it will need to be increased the speed of the compressors to 9920 RPM, so the pressure for both gas lift and gas injection will fulfill the minimum pressure requirements. Discharging the lift gas from the second stage and the injection gas from the third as it was considered in the original design.

Since decreasing the speed of the compressor to 8872 RPM is the scenario selected as best alternative, all three problems stated at the beginning of this analysis were solved, plus reducing the total power consumption in 12% without affecting negatively the electricity production of the waste heat recovery unit

.

## Chapter 6. Conclusions

The intention of this study was to maximize the oil production of the Eldfisk field. Two major constraints were encountered limiting the amount of gas that can be injected into the wells. Given these limitations an economic optimum approach was taken.

The development of a useful tool that permits the calculation of the theoretical optimum gas injection rate for a gas lift well is a valuable approach, since it can allow maximizing the oil production of any well. For learning purposes there is an additional benefit if it is coded in a programming language (MatLab in this case) because all the theory behind any commercial software is also learned and understood.

The developed approach for the calculation of the optimum gas lift injection rate has proved to be more efficient than the conventional method since it needs fewer data points for estimation and also the accuracy when calculating the optimum point is higher than the conventional method.

The best and simplest way to estimate the economic optimum or another type of flowing condition for different lift gas injection rates is the gas lift performance curve.

An increase in the water cut percentage has a direct effect on the volumes that can be produced related to the volume rates of gas that should be injected. For this particular field, the results of the simulations indicate that for the given increments of water cut in the wells, when trying to keep the oil production rates constant, the requirements of gas will increase by 14%. This increment will only be sustained when Eldfisk 2/7 S comes online due to the fact that the actual availability of lift gas is close to the limit.

For the same reason that the lift gas is close to the limit, the optimization of the compression train can only be done at the time being for the existing gas volume rates.

Three aspects of the compression system were the main concern: insufficient discharge pressure, high recirculation rates and low efficiency of the third stage of compression. By reducing the speed of the compressor to 8872 RPM, the third stage of compression was designed to be used as permanent discharge stage for gas lift operations. With this modification the discharge pressure for gas lift operations has been successfully increased to 195 bar, with the only disadvantage that during periods of injection to the reservoir (seldom), it will need to be increased the speed of the compressors to 9920 RPM, so the pressure for both gas lift and gas injection will fulfill the minimum pressure requirements.

Also the recirculation rates have been decreased in every stage. With reductions of 6% in the first stage, 26 % in the second stage and 7% in the third stage, the scrubbers will operate more efficiently and the probability of carrying over liquids will be reduced.

Finally the total power consumption of the compression unit was reduced making the compression system a more efficient unit.

## References

1. **ConocoPhillips Norge.** [Online] January 2012.  
<http://www.conocophillips.no/EN/Norwegian%20shelf/Ekofisk/Eldfisk/Pages/index.aspx>.
2. **Norwegian Petroleum Directorate.** [Online] January 2012.  
<http://www.npd.no/engelsk/cwi/pbl/en/field/all/43527.htm>.
3. **Schlumberger.** *GAS LIFT DESIGN AND TECHNOLOGY.* 2000.
4. **Brown, Kermit E.** *The Technology of Artificial Lift Methods.* Tulsa, Oklahoma : PennWell Publishing CVompany, 1980. ISBN: 0-87814-119-7.
5. **B. Guo, W. C. Lyons, A Ghalambor.** *Petroleum Production Engineering.* s.l. : Elsevier Science & Technology, 2007. ISBN: 0750682701.
6. **G. Forero, K. McFadyen.** *Artificial Lift Manual.* The Hague : SHELL INTERNATIONALE PETROLEUM, December, 1993.
7. **Michael J. Economides, A. Daniel Hill, Christine Ehlig-Economides.** *Petroleum Production Systems .* s.l. : Prentice Hall PTR, 1994. ISBN: 0-13-658683-X.
8. **J.V. Vogel, Shell Oil Co.** *Inflow Performance Relationships for Solution-Gas Drive Wells .* Bakersfield, California : Society of Petroleum Engineers , January 1968. SPE 1476-PA.
9. **Fetkovich, M.J.** *The Isochronal Testing of Oil Wells.* Presented at Las Vegas Technical confrence and exhibition : Societyof Petroleum Engineers, 1973. SPE 4529.
10. **Jones, Lloyd G., Blount, E.M., Mobil Research and Development Corp. and Glaze, O.H., Mobil Oil Corp.** *Use of Short Term Multiple Rate Flow Tests To Predict Performance of Wells Having Turbulence.* SPE Annual Fall Technical Conference and Exhibition, 3-6 October 1976, New Orleans, Louisiana : Society of Petroleum Engineers, 1976. SPE 6133-MS.
11. **Beggs, H. Dale.** *Gas Production Operations.* Oklahoma : OGCI Publications, 1984. ISBN: 0-930972-06-6.
12. **A. Rashid Hasan, C. S. Kabir.** *Fluid Flow and Heat Transfer in Wellbores.* s.l. : Society of Petroleum Engineers, 2002. ISBN: 9781555630942.
13. **Ramey Jr., H.J., Mobil Oil Co.** *Wellbore Heat Transmission .* s.l. : Society of Petroleum Engineers , April 1962. SPE 96-PA.
14. **Chiu, K., Thakur, S.C., Amoco Production Co.** *Modeling of Wellbore Heat Losses in Directional Wells Under Changing Injection Conditions.* SPE Annual Technical Conference and Exhibition, 6-9 October 1991, Dallas, Texas : Society of Petroleum Engineers , 1991. SPE 22870-MS.

15. **I.N. Alves, F.J.S. Alhanati, Ovadia Shoham.** *A Unified Model for Predicting Flowing Temperature Distribution in Wellbores and Pipelines.* s.l. : SPE 20632, 1992.
16. **A. Romero, D. Zhu, and A.D. Hill, SPE, Texas A&M U.** *Temperature Behavior in Multilateral Wells-Application to Intelligent Well.* SPE Latin American and Caribbean Petroleum Engineering Conference, 20-23 June 2005, Rio de Janeiro, Brazil : Society of Petroleum Engineers , 2005. SPE 94982-MS.
17. **B. Moradi, M. Bt. Awang, M. A. Shoushtari.** *Pressure Drop Prediction in Deep Gas Wells.* Malaysia : SPE 147813, 2011.
18. **Maurer Engineering Inc.** *Multiphase Flow Production Model.* Texas : s.n., January 1994.
19. **Beggs, D.H., U. of Tulsa and Brill, J.P., U. of Tulsa.** *A Study of Two-Phase Flow in Inclined Pipes .* s.l. : Society of Petroleum Engineers, May 1973. SPE 4007-PA.
20. **Espanol, J.H., Superior Oil Co., Holmes, C.S., Cities Service Oil Co. and Brown, K.E., U. of Tulsa.** *A Comparison of Existing Multiphase Flow Methods for the Calculation of Pressure Drop in Vertical Wells.* Fall Meeting of the Society of Petroleum Engineers of AIME, 28 September-1 October 1969, Denver, Colorado : Society of Petroleum Engineers , 1969. SPE 2553-MS.
21. **G. A. Gregory, M. Fogarasi and K. Aziz, University of Calgary Calgary, Alberta.** *Analysis of Vertical Two-phase Flow Calculations: Crude Oil-gas Flow In Well Tubing.* 1980 : Petroleum Society of Canada, Canada. SPE 80-01-07.
22. **Beggs, Dale.** *Production Optimization.* Tulsa, Oklahoma : OGCI, Inc., Petroskills, 2002. ISBN: 0-930972-14-7.
23. **Barrufet, Maria A., Rasool, Ahmed, Petroleum Engineering Department, Texas A&M University 77843-3116 and Aggour, Mohamed, King Fahd U. of Petroleum & Minerals, Daharan 31261, Saudi Arabia.** *Prediction of Bottomhole Flowing Pressures in Multiphase Systems Using a Thermodynamic Equation of State.* SPE Production Operations Symposium, 2-4 April 1995, Oklahoma City, Oklahoma : Society of Petroleum Engineers , 1995. SPE 29479-MS.
24. **D. Peng, D. B. Robinson.** *A new Two-Constant Equation of State.* Alberta, Canada : Ind. Eng. Chem., 1975. Vol. 15.
25. **A. L. Lee, M.H. Gonzales and B.E. Eakin.** *The Viscosity of Natural Gases.* s.l. : JPT, 1966.
26. **A.F. Bertuzzi, J.K. Welchon, and F.H. Poettmann, Phillips Petroleum Co.** *Description and Analysis of an Efficient Continuous-Flow Gas-Lift Installation.* s.l. : Society of Petroleum Engineers , November 1953. ISSN: 0149-2136.



27. **W.E. Gilbert, N.V.De Bataafsche Petroleum Maatschippj.** *Flowing and Gas-lift well Performance*. s.l. : Flowing and Gas-lift well Performance, 1954. API 54-126.
28. **Gopinath, Halder.** *Introduction to Chemical Engineering Thermodynamics*. New Delhi : PHI Learning Pvt. Ltd., 2009. ISBN: 978-81-203-3846-3.
29. **Devold, Håvard.** *Oil and Gas Production Handbook*. Oslo : ABB ATPA Oil an Gas, June 2006.
30. **Howard G .Murphy, Jr.** *COMPRESSOR PERFORMANCE MODELING TO IMPROVE EFFICIENCY AND THE QUALITY OF OPTIMIZATION DECISIONS*. El Paso, Texas : Pipeline Simulation Interest Group, 1989.
31. **Bloch, H.P. and Hoefner, J.J.** *Reciprocating Compressors, Operation and Maintenance*. . s.l. : Gulf Professional Publishing. , 1996. ISBN 0-88415-525-0..
32. **Aungier, Ronald H.** *Centrifugal Compressors A Strategy for Aerodynamic design and Analysis*. . s.l. : ASME Press., 2000. ISBN 0-7918-0093-8..
33. **Office, Sustainable Development.** *Compressed Air Systems*. Australia : Government of Western Australia, 2002.
34. **Perry, R.H. and Green, D.W.** *Perry's Chemical Engineers' Handbook (8th ed.)*. s.l. : McGraw Hill., 2007. ISBN 0-07-142294-3.
35. **Gas Processors Suppliers Association.** *Engineering Data Book, 11th Edition*. Tulsa, Oklahoma : Gas Processors Association, 1998.
36. **Hanlon, Paul C.** *Compressor Handbook*. New York : McGraw-Hill, 2001. ISBN: 0-07-026005-2.

## Nomenclature

Area= inside cross section area of the tubing  $m^2$   
 C=Coefficient  
 D=diameter (m)  
 Dtubi=inside diameter of tubing  
 GLR<sub>f</sub>= Formation oil GLR,  $L^3/L^3$   
 GLR<sub>inj</sub>= Injection GLR,  $L^3/L^3$   
 GLR<sub>opt</sub>= optimum GLR at operating flow rate,  $L^3/L^3$   
 L=length (m)  
 L1, L2, L3, L4= Correlation boundaries  
 N<sub>FR</sub>= Froude Number  
 N<sub>IV</sub>=Liquid velocity number  
 P=Pressure (Pa)  
 P<sub>c</sub>= Critical Pressure (Pa)  
 Pr=Prandtl Number (Dimensionless)  
 Pr=Reservoir Pressure (Pa)  
 P<sub>wf</sub>= Flowing Bottomhole Pressure (Pa)  
 Q= Heat Flow Rate (J/s)  
 Q<sub>omax</sub>=Maximum Liquid Production rate  $m^3/s$   
 R= Universal Gas Constant (8.31 J/(mol·K))  
 Re= Reynolds Number (Dimensionless)  
 S= Correlation factor  
 T= Temperature (K)  
 T<sub>c</sub>= Critical Temperature (K)  
 U<sub>to</sub>=Overall heat transfer coefficient (W/m<sup>2</sup>-K)  
 V= volume (m<sup>3</sup>)  
 Y<sub>1</sub>=Hold-up at angle  $\theta$   
 Y<sub>10</sub>=Horizontal Hold-up  
 Z= compressibility factor of the gas  
  
 ṁ= Mass Flow rate (Kg/s)  
 a(t)=attraction parameter  
 b= Van der Waals co-volume  
 c<sub>p</sub>= Specific heat of the gas (J/Kg-K)  
 $\left(\frac{dP}{dz}\right)_f$  = Pressure drop due to friction (Pa/m)  
 $\left(\frac{dP}{dz}\right)_{el}$  = Pressure drop due to elevation (Pa/m)  
 $\left(\frac{dP}{dz}\right)_{ac}$  = Pressure drop due to acceleration (Pa/m)  
 f=Moody's friction factor  
 f<sub>n</sub>= no slip friction factor based on smooth pipe  
 f<sub>tp</sub>= Two phase friction factor  
 g= Acceleration of gravity (m/s<sup>2</sup>)

h=enthalpy of the fluid  
 h<sub>c</sub>= Heat transfer coefficient due to convection (W/m<sup>2</sup>-K)  
 h<sub>f</sub>= Heat transfer coefficient of the fluid (W/m<sup>2</sup>-K)  
 h<sub>r</sub>= Heat transfer coefficient due to radiation (W/m<sup>2</sup>-K)  
 k=thermal conductivity (W/m-K)  
 m=constant characteristic of each substance  
 q<sub>g,inj</sub>=Gas injection rate  $sm^3/d$   
 q<sub>o</sub>, q<sub>l</sub> =oil or liquid production rate  $m^3/d$   
 r=radius (m)  
 t= Time (s)  
 t<sub>D</sub>= Dimensionless time  
 u= velocity of the fluid  
 u<sub>m</sub>= Mixture velocity m/s  
 u<sub>sg</sub>= Gas superficial Velocity m/s  
 u<sub>sl</sub>= Liquid superficial Velocity m/s

### Greek Symbols

α(T)=Dimensionless function of reduced temperature and eccentric factor  
 β= Coefficient of Volume Expansion (1/K)  
 Δz=Length of the segment (m)  
 ε= Roughness of the pipe (m)  
 η= Joule-Thompson Coefficient  
 θ=Angle of deviation from the horizontal (degrees)  
 λ<sub>l</sub>=No slip liquid fraction  
 μ=Viscosity (Pa-s)  
 μ<sub>mns</sub>=No-slip mixture viscosity (Pa-s)  
 ρ<sub>g</sub>=Gas density (Kg/m<sup>3</sup>)  
 ρ<sub>l</sub>=Liquid density (Kg/m<sup>3</sup>)  
 ρ<sub>mns</sub>=No-slip mixture density (Kg/m<sup>3</sup>)  
 ρ<sub>tp</sub>=Two phase density (Kg/m<sup>3</sup>)  
 σ=interfacial tension  
 φ= Dimensionless Correction Parameter  
 Ψ= Inclination Correction factor  
 ω= Eccentric factor

### Beggs and Brill Arbitrary Constants

a, b, c, d, e, f, g, A, B

## Appendix A – Graphic results of the Simulations

### i. Well A-01

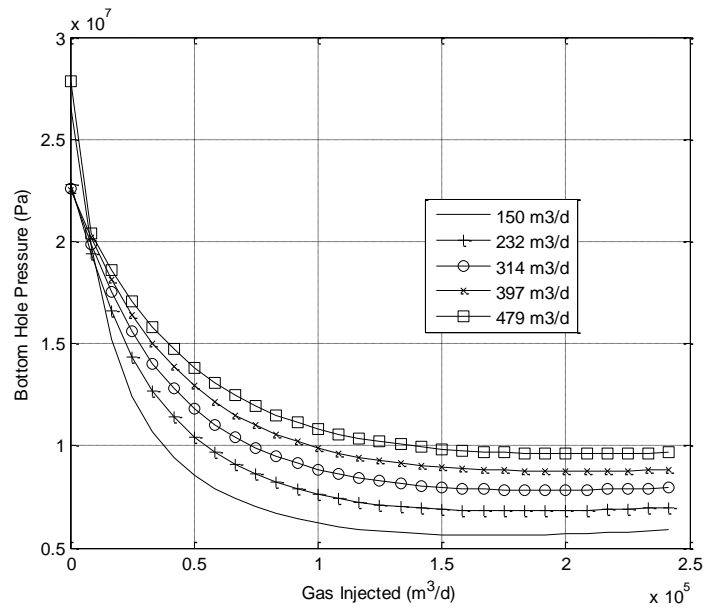


Figure A-1: VLP curves for Well A-01

By taking the minimum values of each curve it is possible to create the optimum VLP curve.

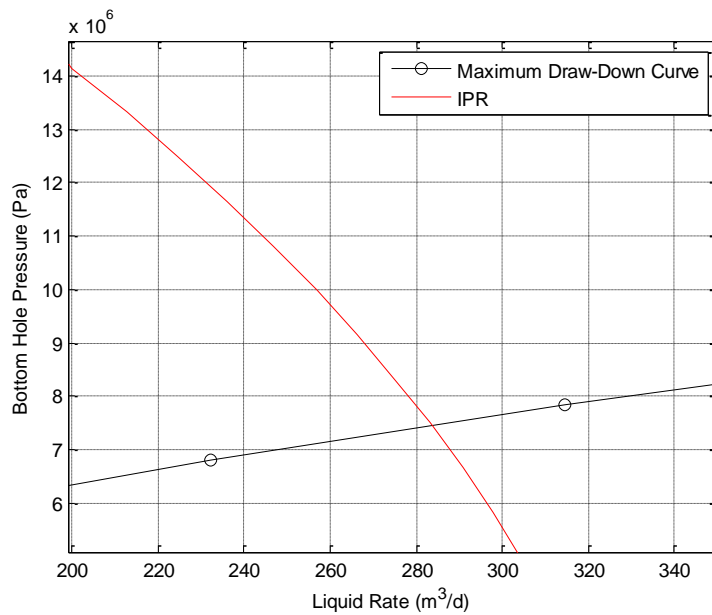


Figure A-2: VLP vs. IPR for well A-01

From the previous two figures the optimum gas injection rate is 188470 m<sup>3</sup>/d, allowing a maximum oil production rate of 283 m<sup>3</sup>/d.

ii. Well A-02

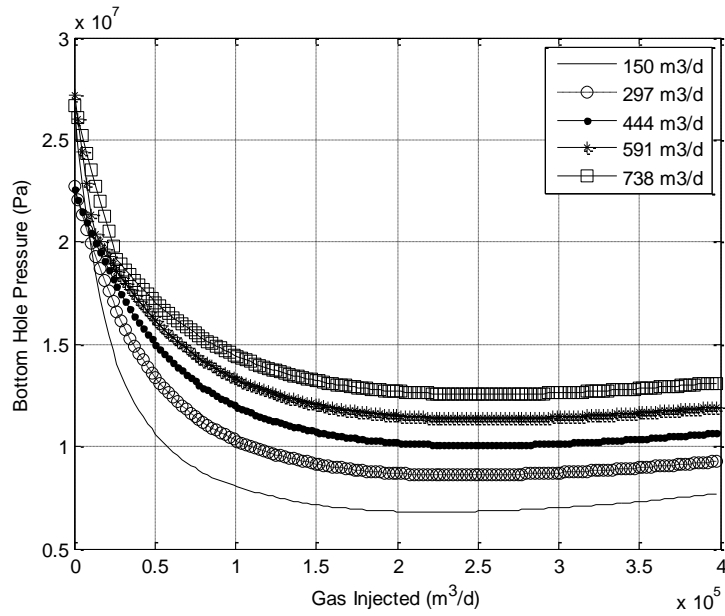


Figure A-3: VLP curves for Well A-02

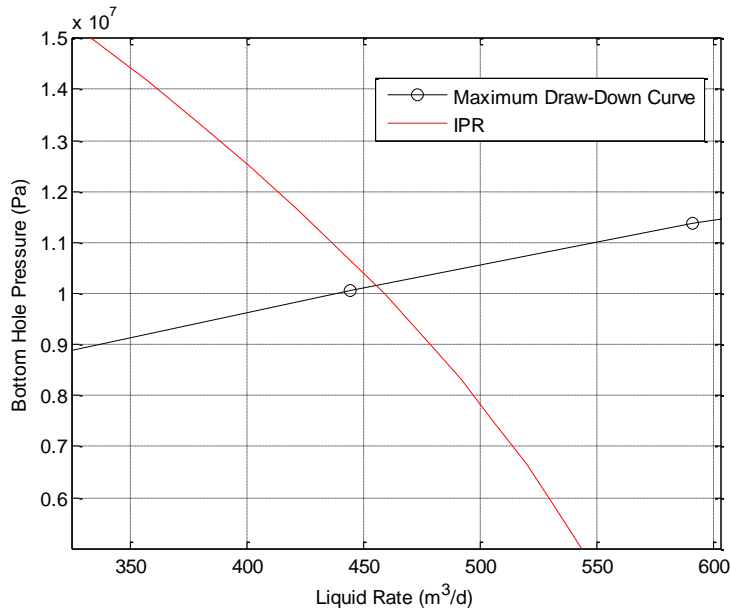


Figure A-4: VLP vs. IPR for well A-02

From the previous two figures the optimum gas injection rate is  $250800 m^3/d$ , allowing a maximum oil production rate of  $455 m^3/d$ .

iii. Well A-03

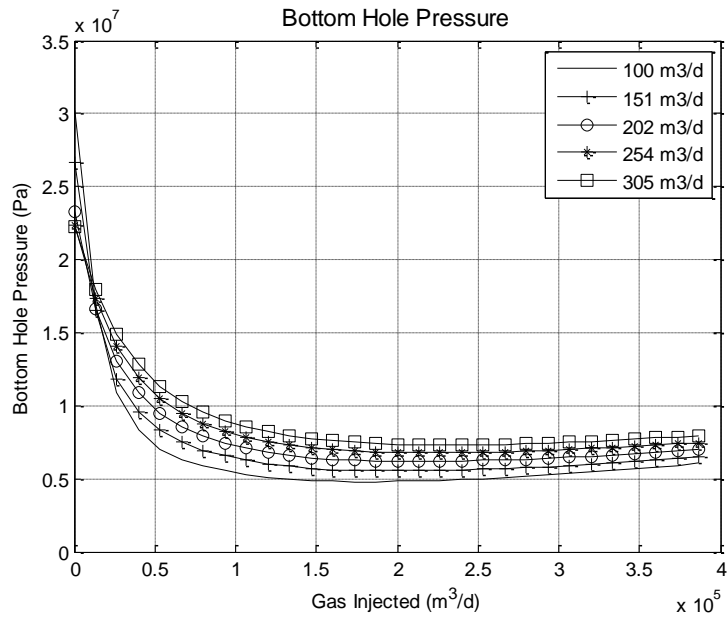


Figure A-5: VLP curves for Well A-03

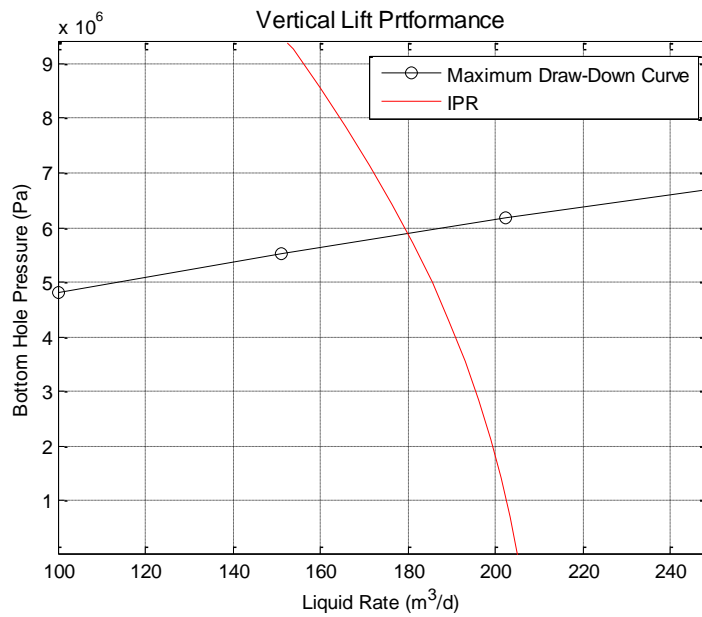


Figure A-6: VLP vs. IPR for well A-03

From the previous two figures the optimum gas injection rate is 207500 m<sup>3</sup>/d, allowing a maximum oil production rate of 180 m<sup>3</sup>/d.

iv. Well A-10

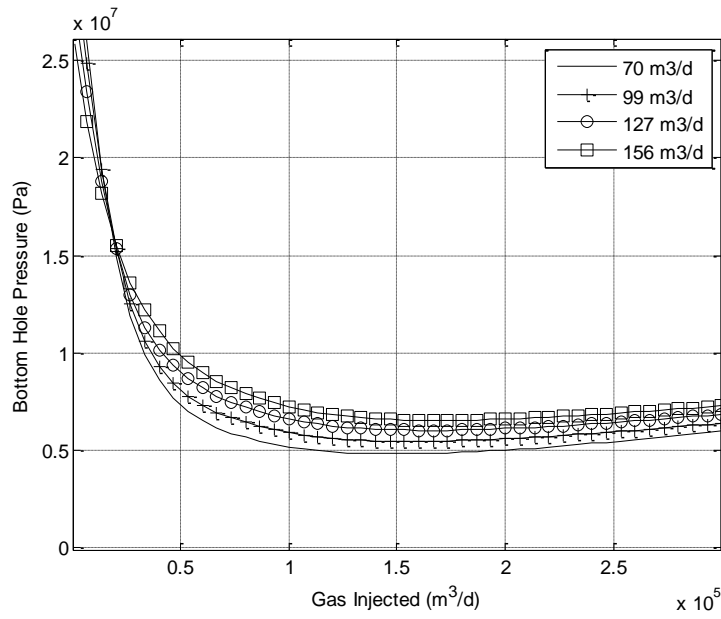


Figure A-7: VLP curves for Well A-10

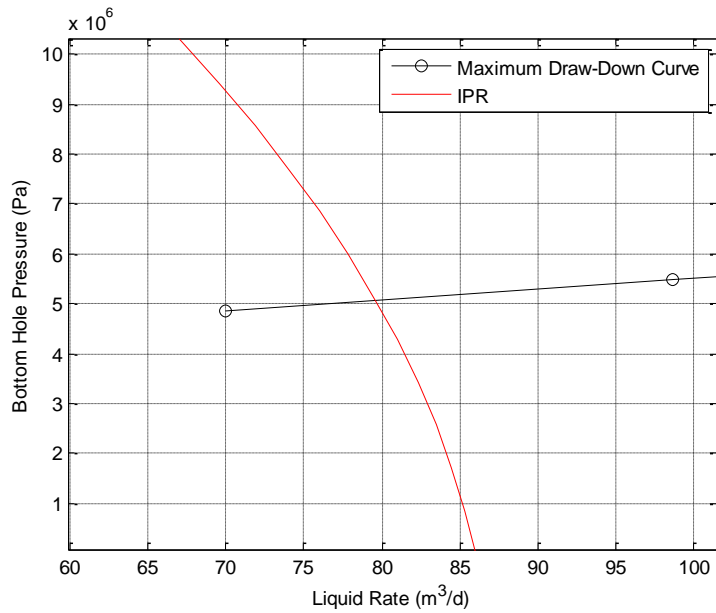


Figure A-8: VLP vs. IPR for well A-10

For well A-10 the optimum gas injection rate is 151145 m<sup>3</sup>/d, allowing a maximum oil production rate of 79.6 m<sup>3</sup>/d.

v. Well A-16

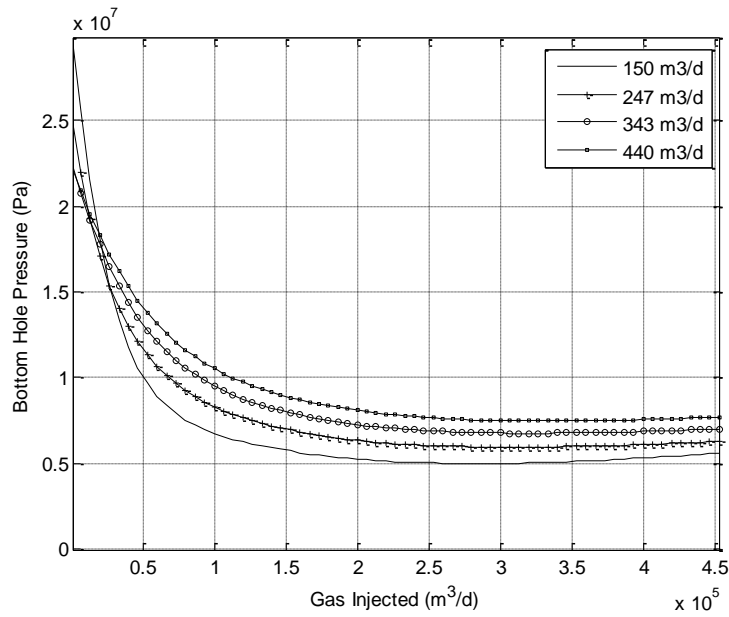


Figure A-9: VLP curves for Well A-16

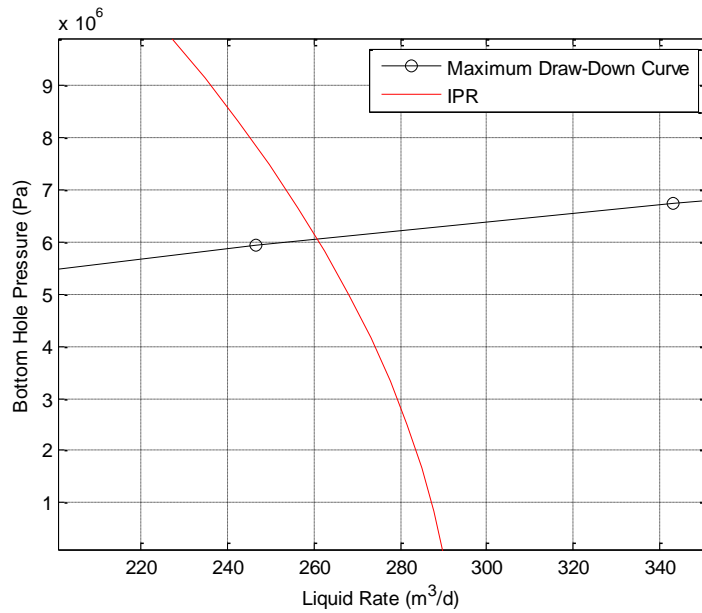


Figure A-10: VLP vs. IPR for well A-16

The optimum gas injection rate for well A-16 is 302910 m<sup>3</sup>/d, allowing a maximum oil production rate of 260.75 m<sup>3</sup>/d.

vi. Well A-17

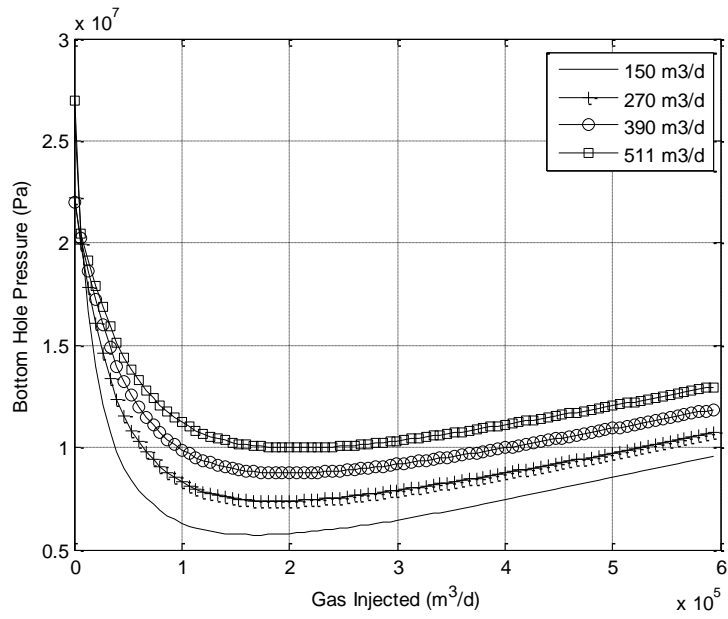


Figure A-11: VLP curves for Well A-17

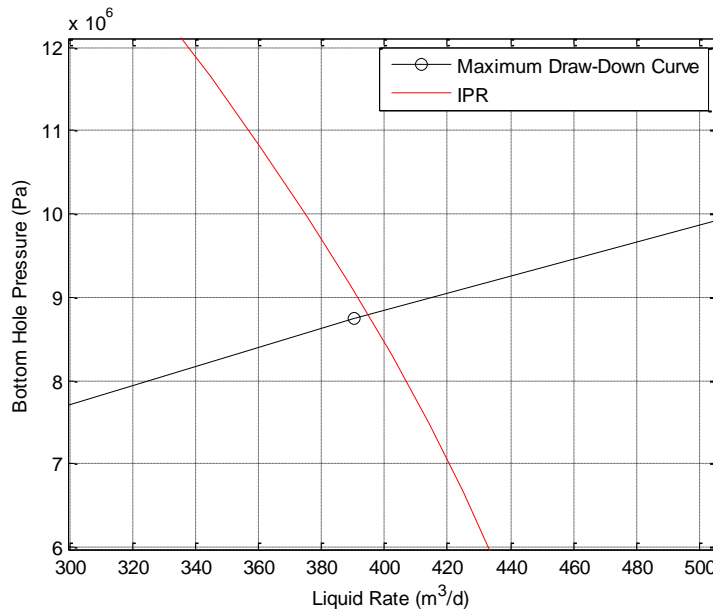


Figure A-12: VLP vs. IPR for well A-17

The optimum gas injection rate for well A-17 is 200190 m<sup>3</sup>/d, allowing a maximum oil production rate of 395 m<sup>3</sup>/d.



vii. Well A-18

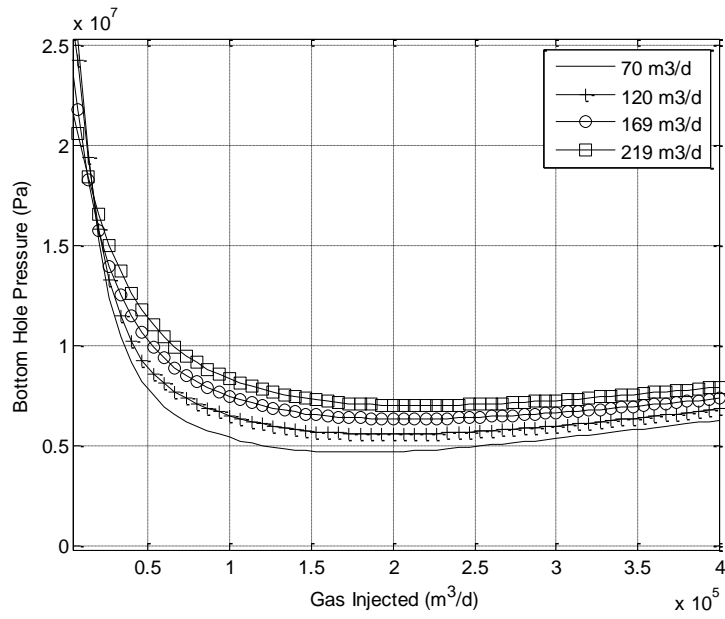


Figure A-13: VLP curves for Well A-18

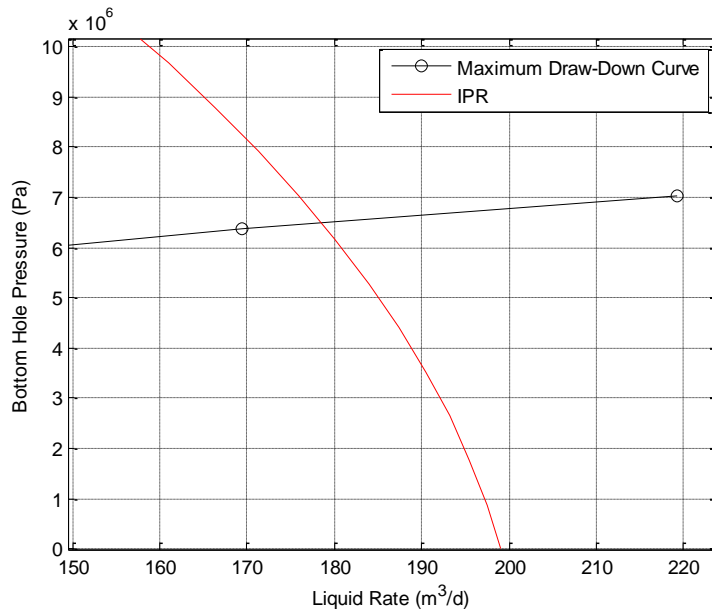


Figure A-14: VLP vs. IPR for well A-18

From the previous two figures the optimum gas injection rate is 207880 m<sup>3</sup>/d, allowing a maximum oil production rate of 178.57 m<sup>3</sup>/d.

viii. Well A-19

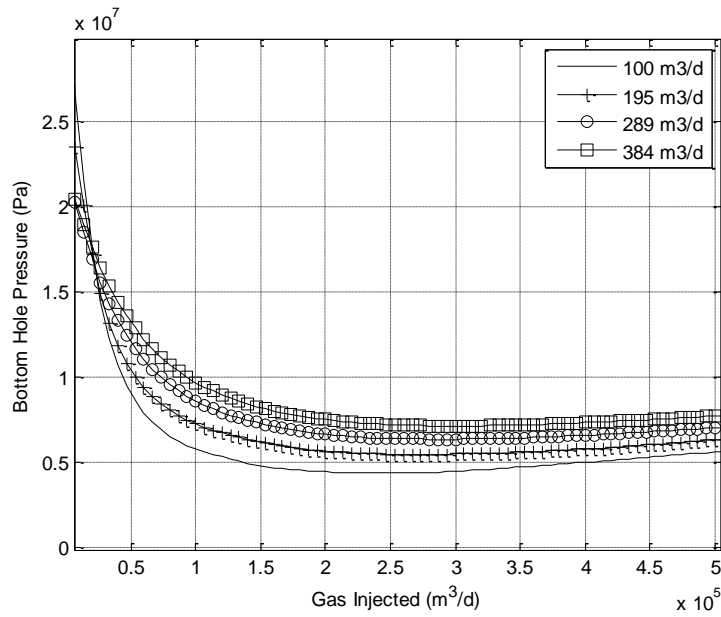


Figure A-15: VLP curves for Well A-19

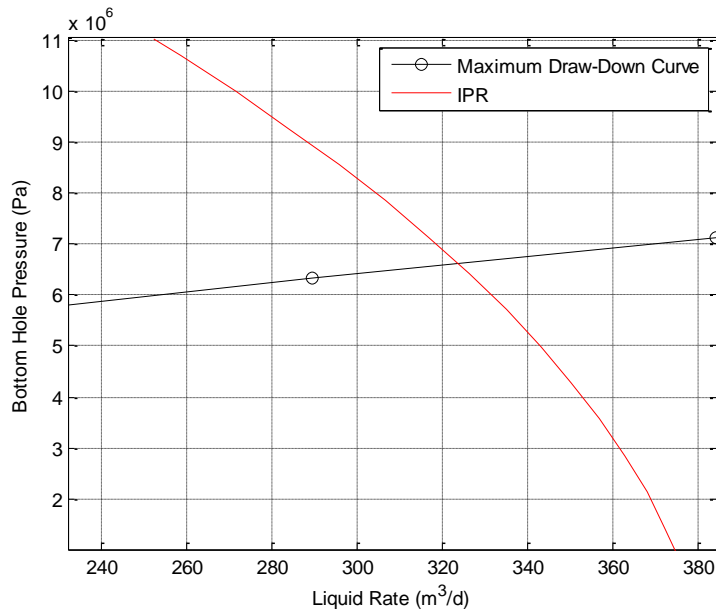


Figure A-16: VLP vs. IPR for well A-19

From the previous two figures the optimum gas injection rate is 295740 m<sup>3</sup>/d, allowing a maximum oil production rate of 324 m<sup>3</sup>/d.

ix. Well A-20

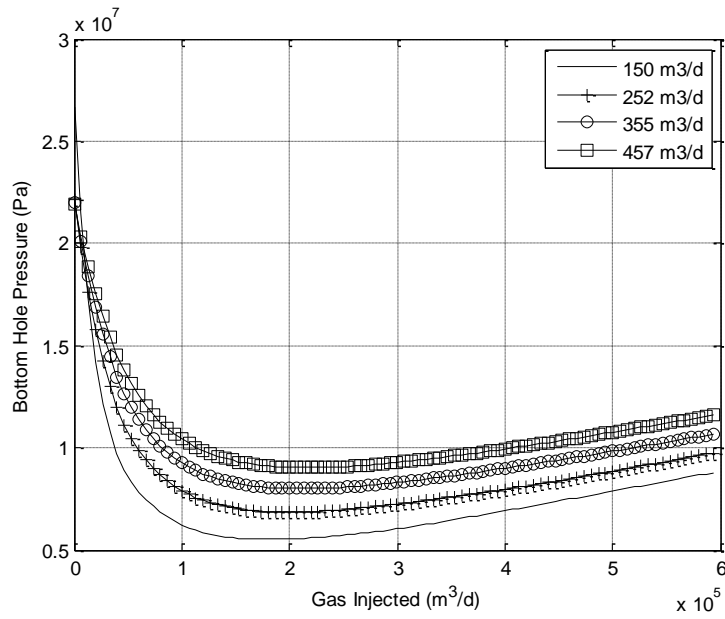


Figure A-17: VLP curves for Well A-20

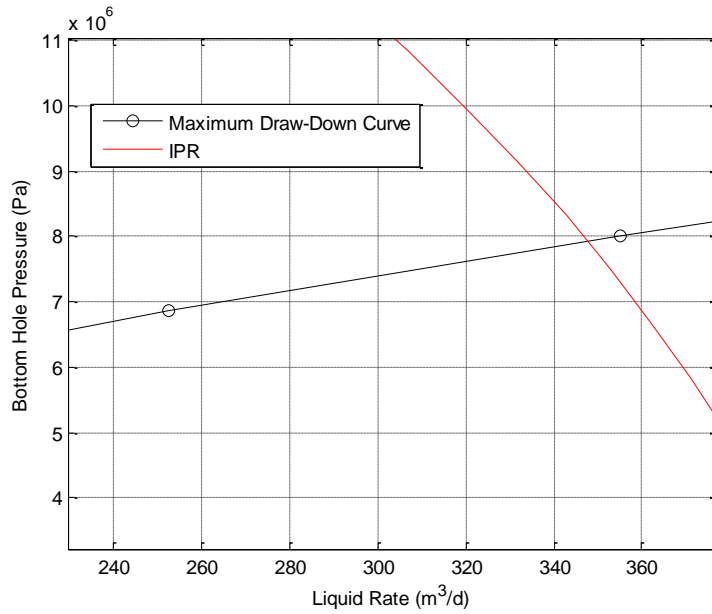


Figure A-18: VLP vs. IPR for well A-20

For well A-20 the optimum gas injection rate is 206190 m<sup>3</sup>/d, allowing a maximum oil production rate of 347.7 m<sup>3</sup>/d.

**x. Well A-23**

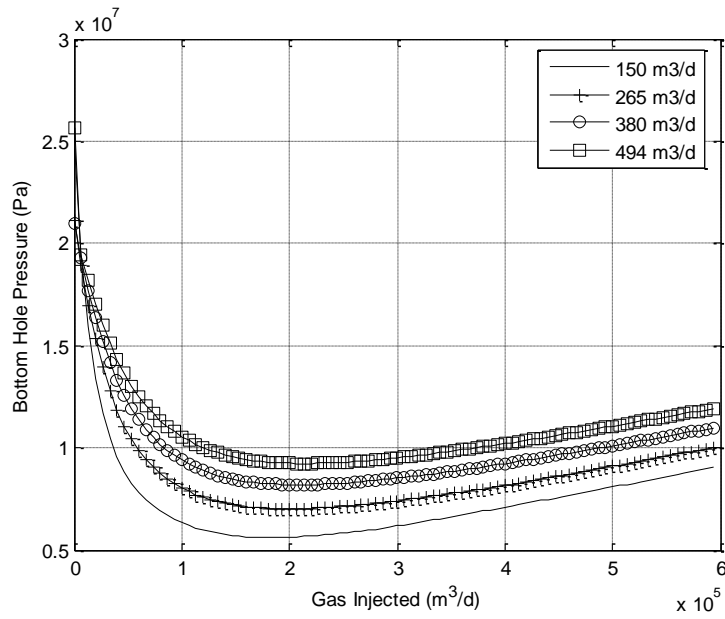


Figure A-19: VLP curves for Well A-23

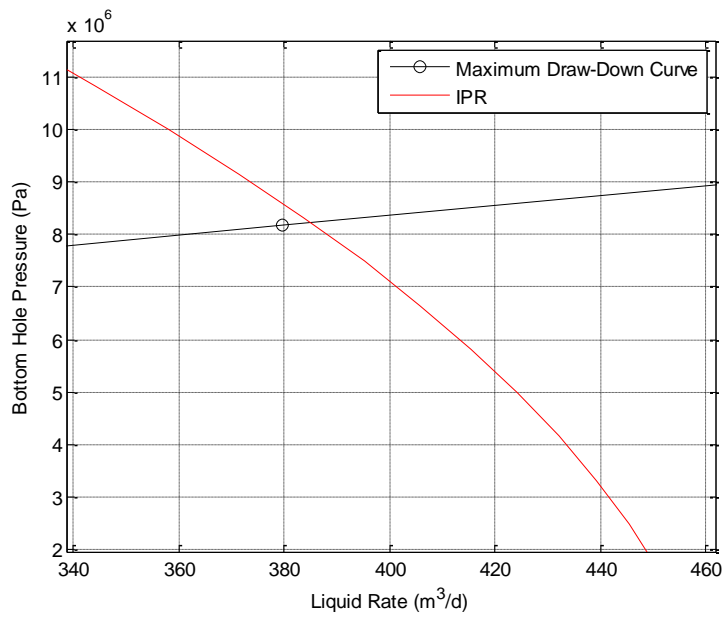


Figure A-20: VLP vs. IPR for well A-23

For well A-23 the optimum gas injection rate is 206980 m<sup>3</sup>/d, allowing a maximum oil production rate of 385 m<sup>3</sup>/d.

## xi. Well A-26

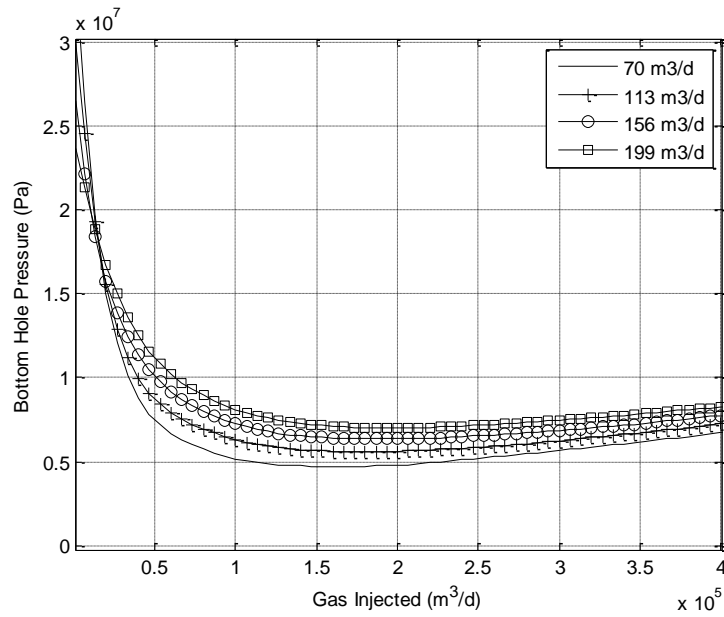


Figure A-21: VLP curves for Well A-26

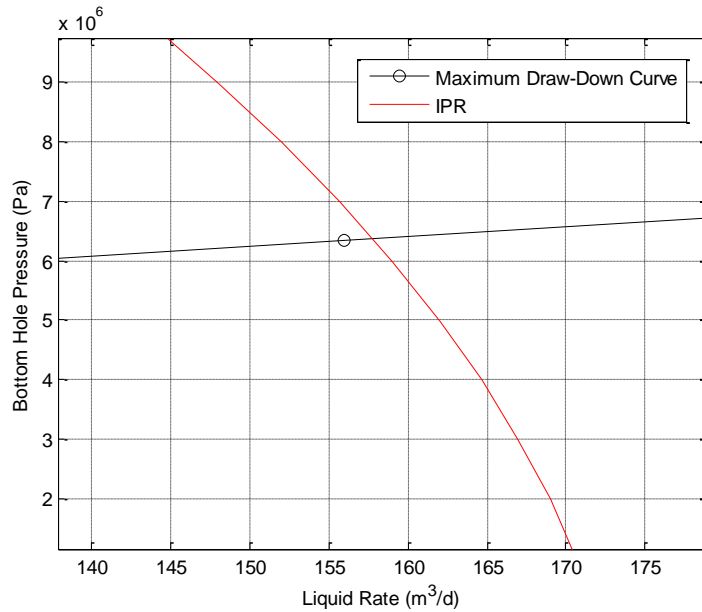


Figure A-22: VLP vs. IPR for well A-26

The optimum gas injection rate for well A-26 is  $186940 m^3/d$ , allowing a maximum oil production rate of  $157.8 m^3/d$ .

xii. Well A-28

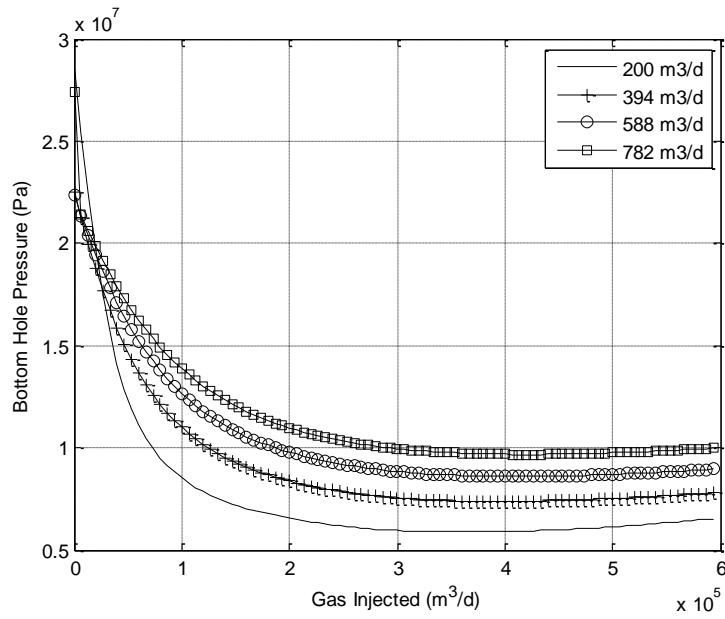


Figure A-23: VLP curves for Well A-28

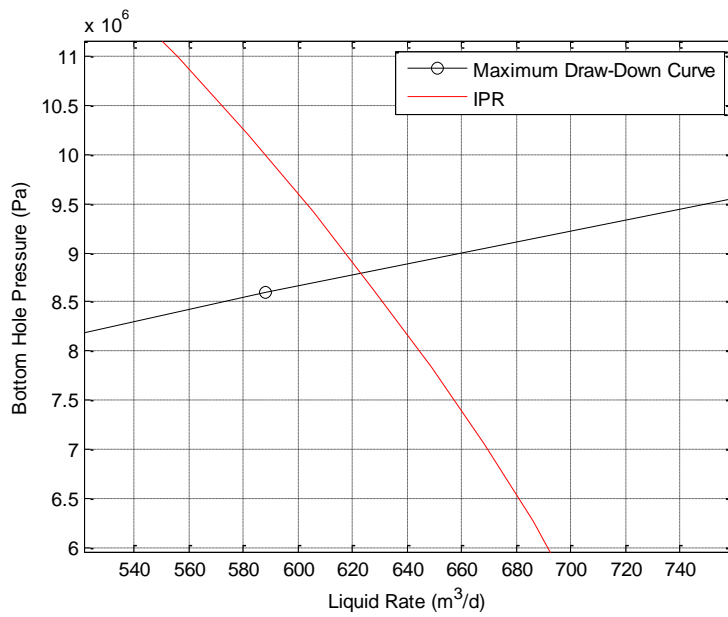


Figure A-24: VLP vs. IPR for well A-28

The optimum gas injection rate for well A-28 is 409070 m<sup>3</sup>/d, allowing a maximum oil production rate of 623 m<sup>3</sup>/d.

xiii. Well B-10

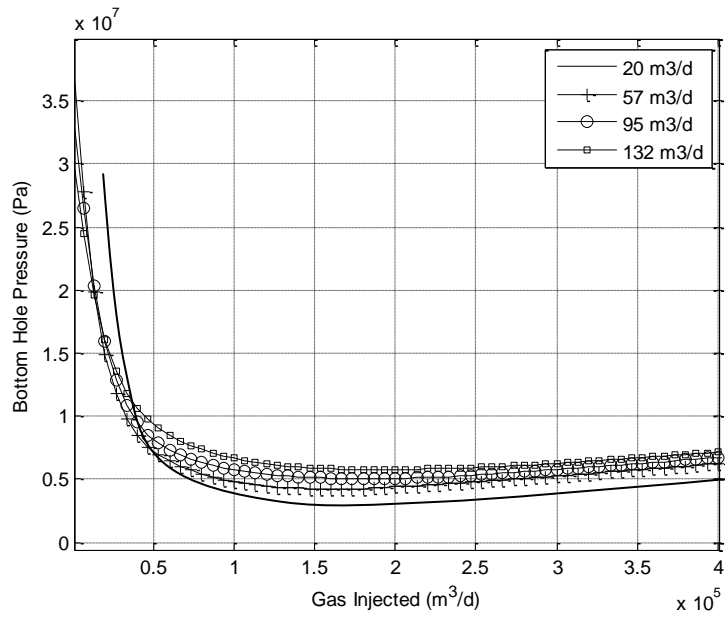


Figure A-25: VLP curves for Well B-10

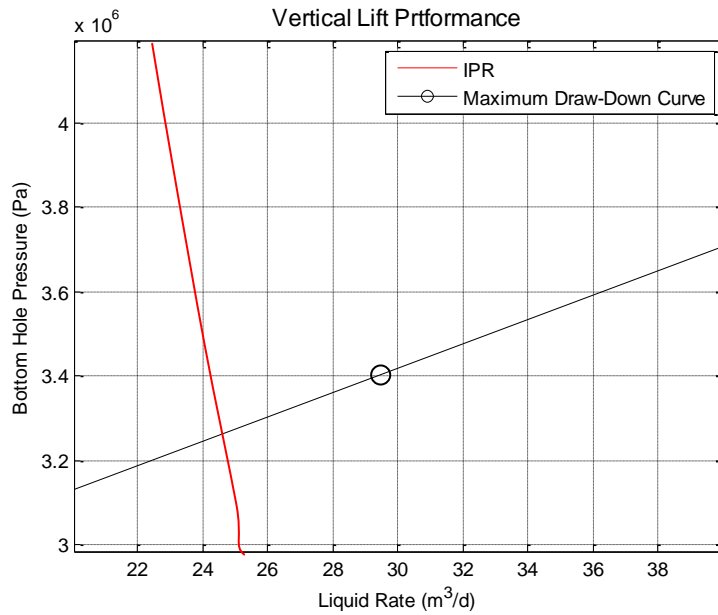


Figure A-26: VLP vs. IPR for well B-10

From the previous two figures the optimum gas injection rate is 227125 m<sup>3</sup>/d, allowing a maximum oil production rate of 24.5 m<sup>3</sup>/d.

xiv. Well B-11

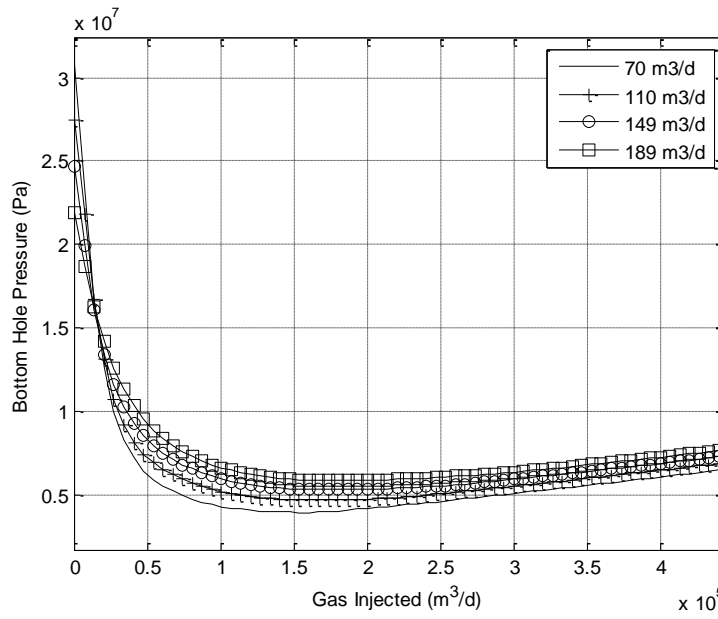


Figure A-27: VLP curves for Well B-11

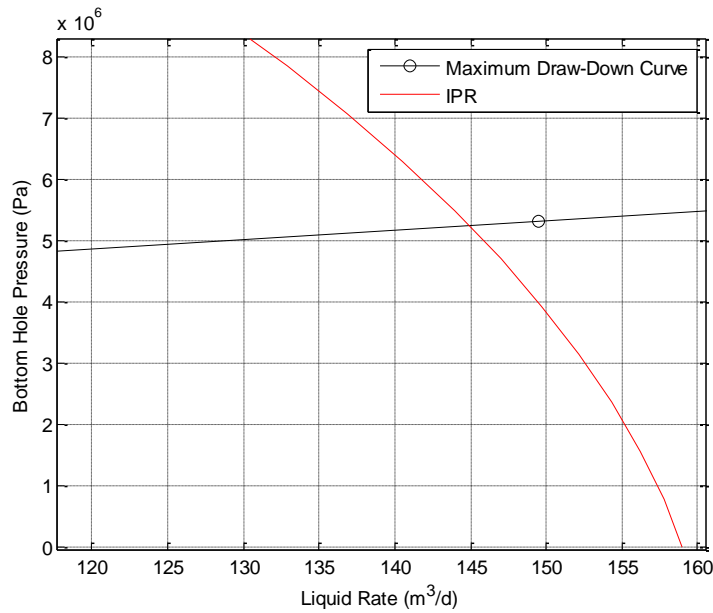


Figure A-28: VLP vs. IPR for well B-11

From the previous two figures the optimum gas injection rate is 172560 m<sup>3</sup>/d, allowing a maximum oil production rate of 144.9 m<sup>3</sup>/d.



xv. Well B-14

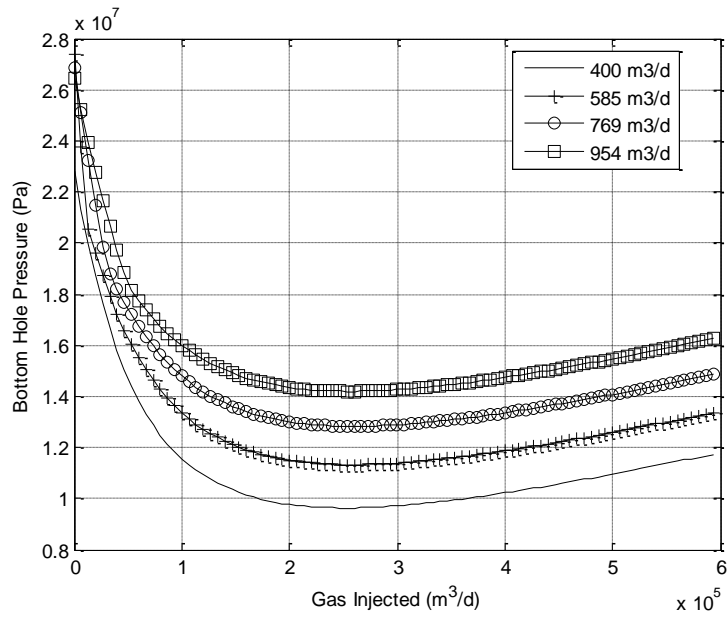


Figure A-29: VLP curves for Well B-14

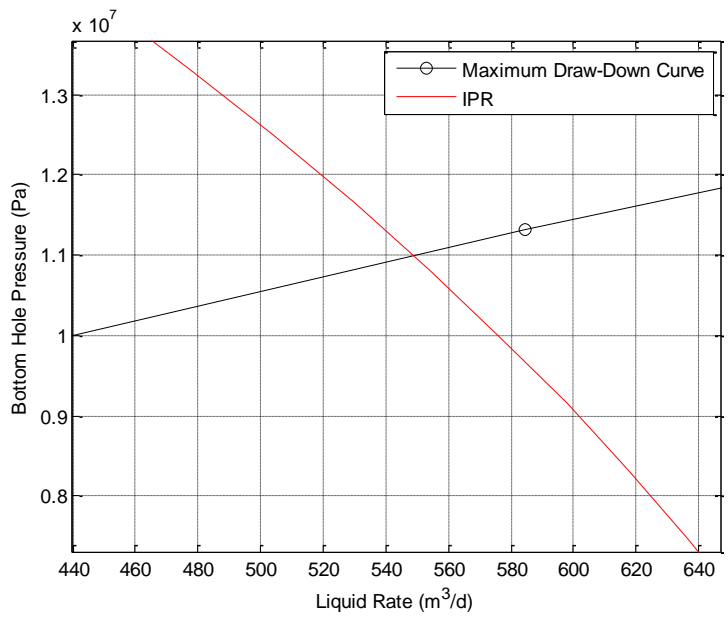


Figure A-30: VLP vs. IPR for well B-14

For well B-14 the optimum gas injection rate is 258670 m<sup>3</sup>/d, allowing a maximum oil production rate of 548 m<sup>3</sup>/d.

xvi. Well B-17

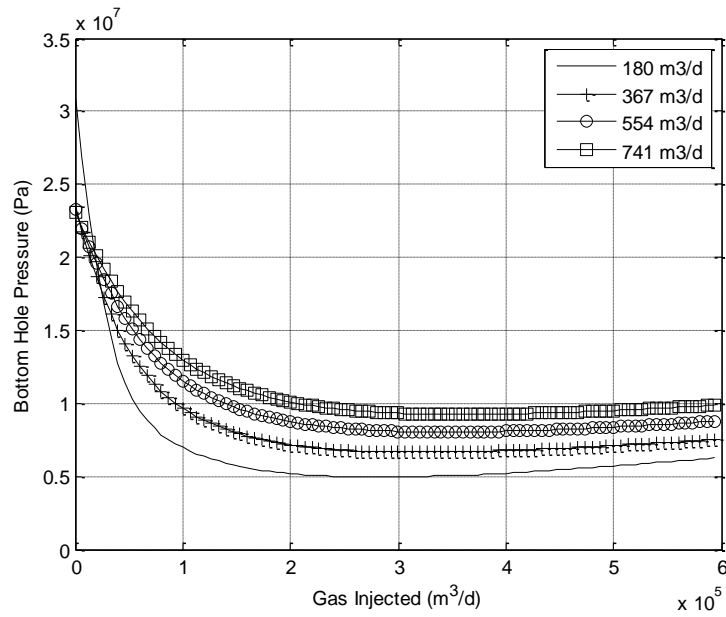


Figure A-31: VLP curves for Well B-17

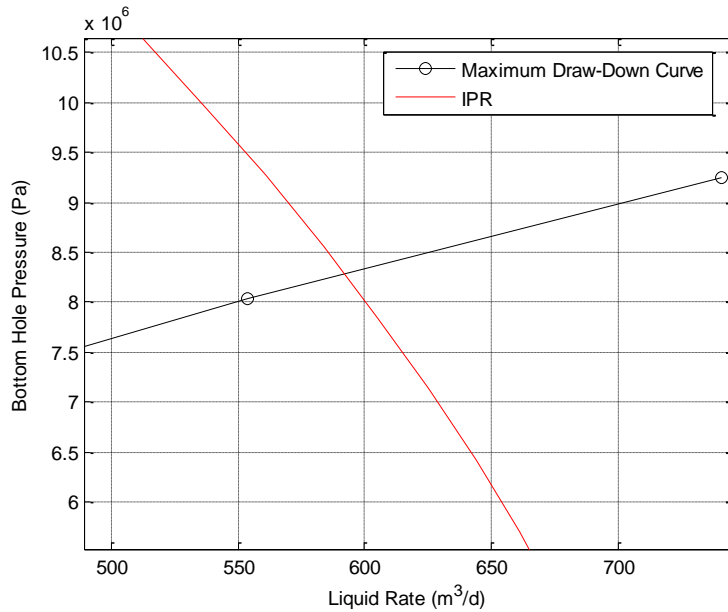


Figure A-32: VLP vs. IPR for well B-17

For well B-17 the optimum gas injection rate is 344050 m<sup>3</sup>/d, allowing a maximum oil production rate of 592 m<sup>3</sup>/d.

xvii. Well B-19

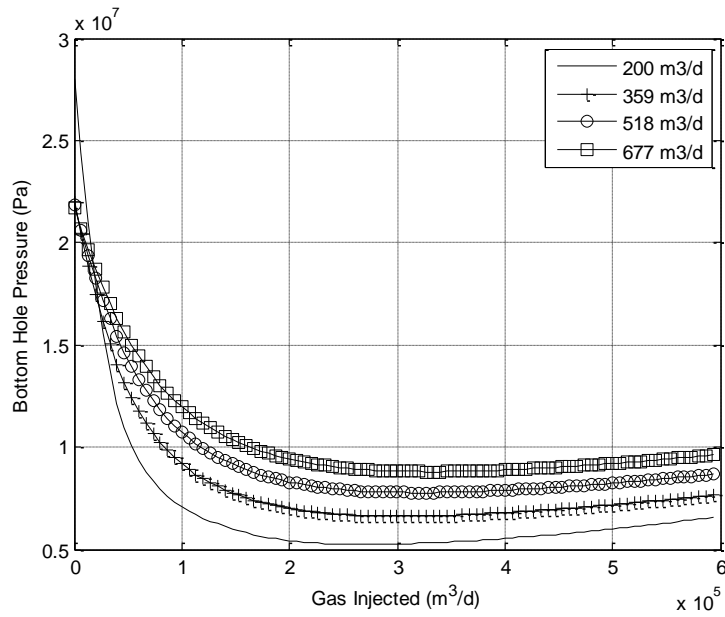


Figure A-33: VLP curves for Well B-19

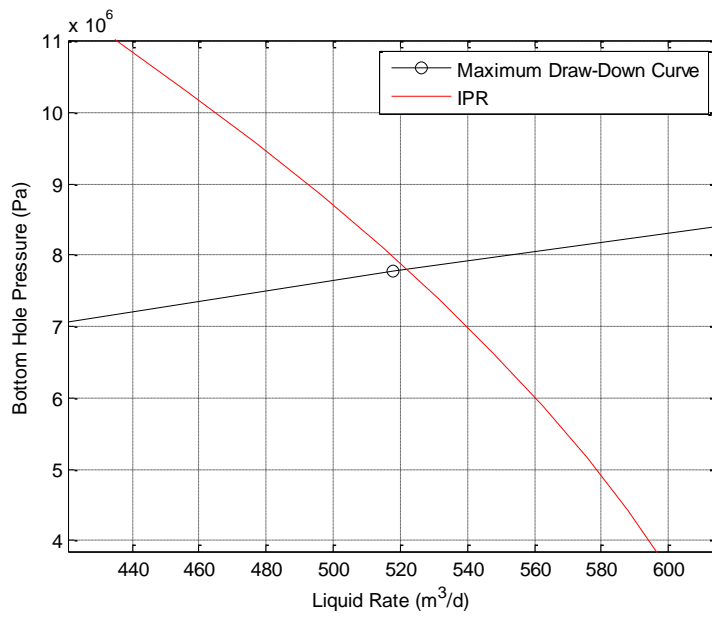


Figure A-34: VLP vs. IPR for well B-19

The optimum gas injection rate for well B-19 is 320320 m<sup>3</sup>/d, allowing a maximum oil production rate of 521.8 m<sup>3</sup>/d.

## Appendix B – Gas Lift Performance Curves

### i. Well A-01

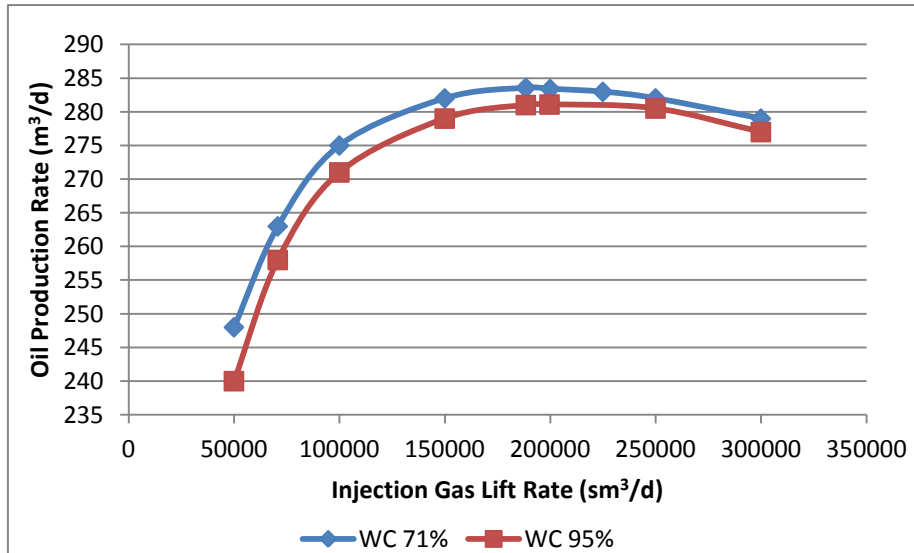


Figure B-1: Gas Lift Performance Curve for Well A-01

The actual water cut of well A-01 is 71%; and the economic optimum is located at 85000 sm<sup>3</sup>/d, which will allow to produce 269 m<sup>3</sup>/d. In the case of an increase in the water cut from 71% to 95 % the volume of gas needed to produce 264 m<sup>3</sup>/d of oil is 85396 sm<sup>3</sup>/d.

### ii. Well A-02

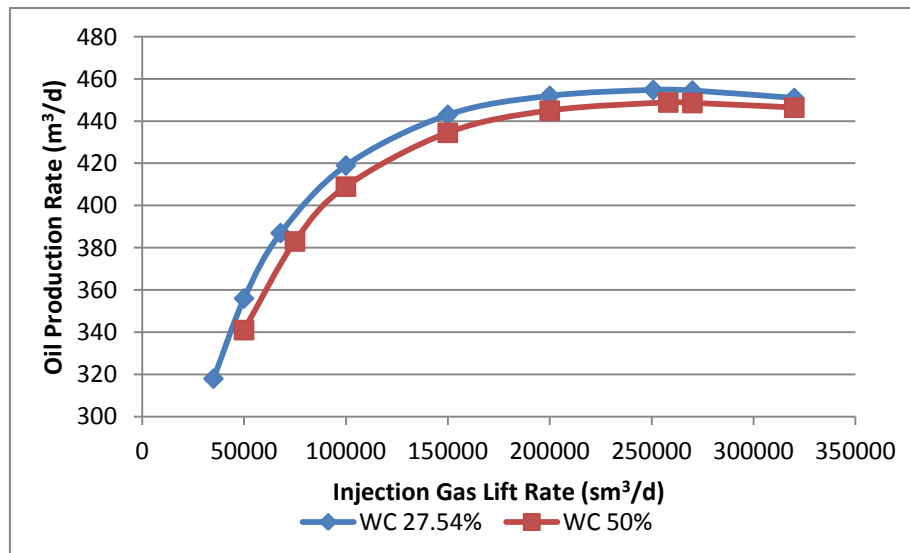


Figure B-2: Gas Lift Performance Curve for Well A-02

The economic optimum for well A-02 is located at 50000 sm<sup>3</sup>/d, which will allow to produce 356 m<sup>3</sup>/d. In the case of an increase in the water cut, the volume of gas needed to produce 389 m<sup>3</sup>/d of oil is 75000 sm<sup>3</sup>/d.

## iii. Well A-03

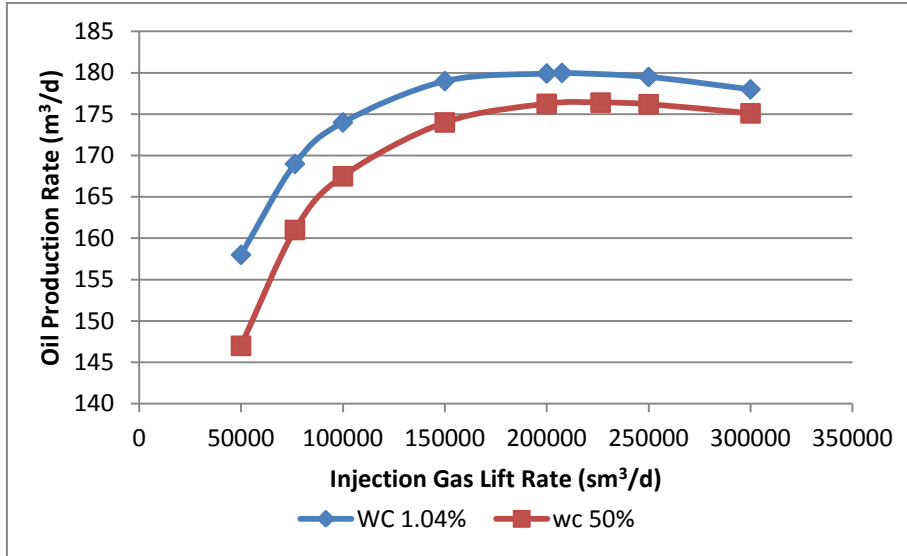


Figure B-3: Gas Lift Performance Curve for Well A-03

The economic optimum for well A-03 is located at 74455 sm<sup>3</sup>/d, which will allow to produce 169 m<sup>3</sup>/d. In the case of an increase in the water cut, the volume of gas needed to produce 161 m<sup>3</sup>/d of oil is 76455 sm<sup>3</sup>/d.

## i. Well A-10

From the following figure the economic optimum for well A-10 is located at 87500 sm<sup>3</sup>/d, which will allow to produce 78 m<sup>3</sup>/d. In the case of an increase in the water cut from 12.19% to 50%, the volume of gas needed to produce 76 m<sup>3</sup>/d of oil is 100000 sm<sup>3</sup>/d.

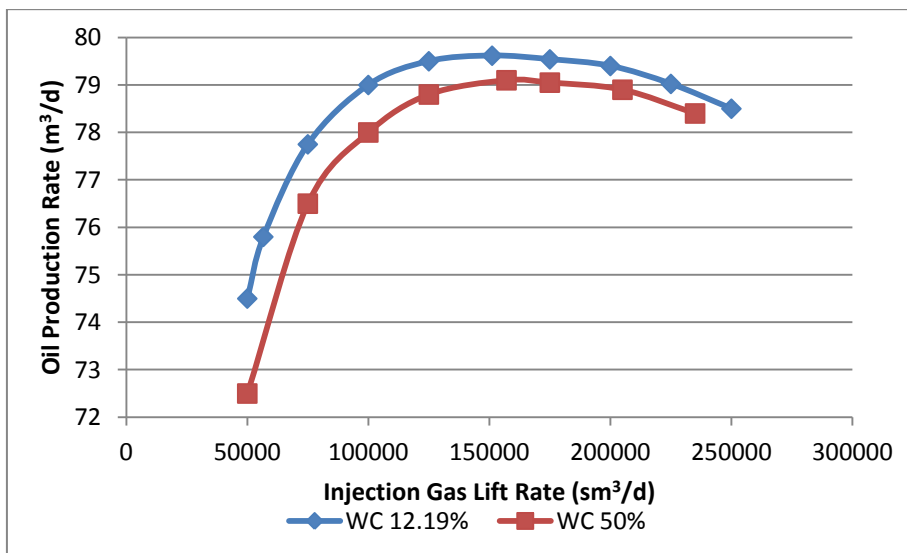


Figure B-4: Gas Lift Performance Curve for Well A-10

ii. Well A-16

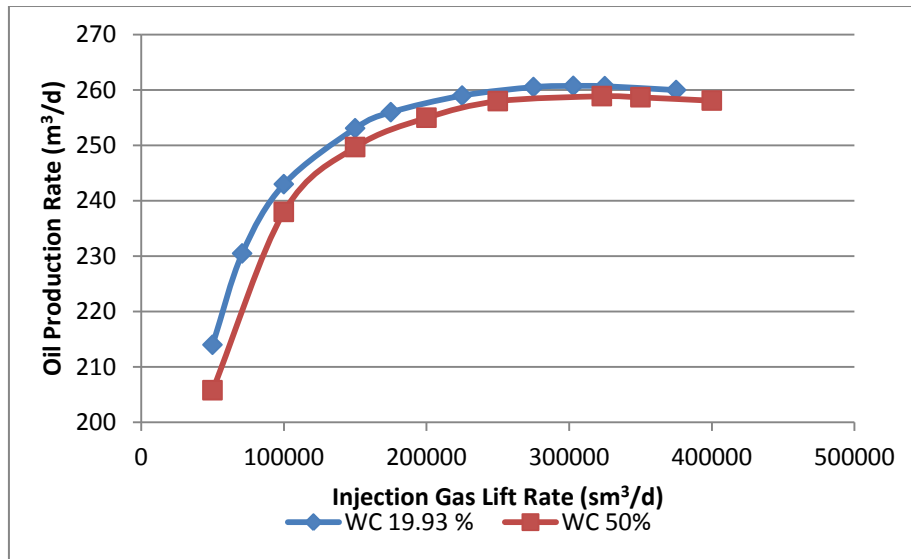


Figure B-5: Gas Lift Performance Curve for Well A-16

The economic optimum for well A-16 is located at 85400 sm<sup>3</sup>/d, which will allow to produce 237 m<sup>3</sup>/d. In the case of an increase in the water cut, the volume of gas needed to produce 238 m<sup>3</sup>/d of oil is 100000 sm<sup>3</sup>/d.

iii. Well A-17

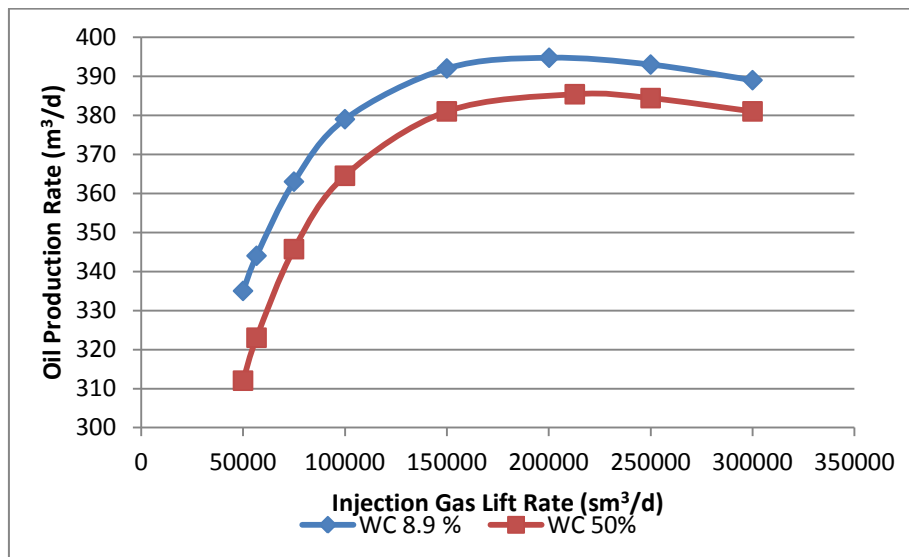


Figure B-6: Gas Lift Performance Curve for Well A-17

The economic optimum for well A-17 is located at 75000 sm<sup>3</sup>/d, which will allow to produce 363 m<sup>3</sup>/d. In the case of an increase in the water cut, the volume of gas needed to produce 360 m<sup>3</sup>/d of oil is 90000 sm<sup>3</sup>/d.

## iv. Well A-18

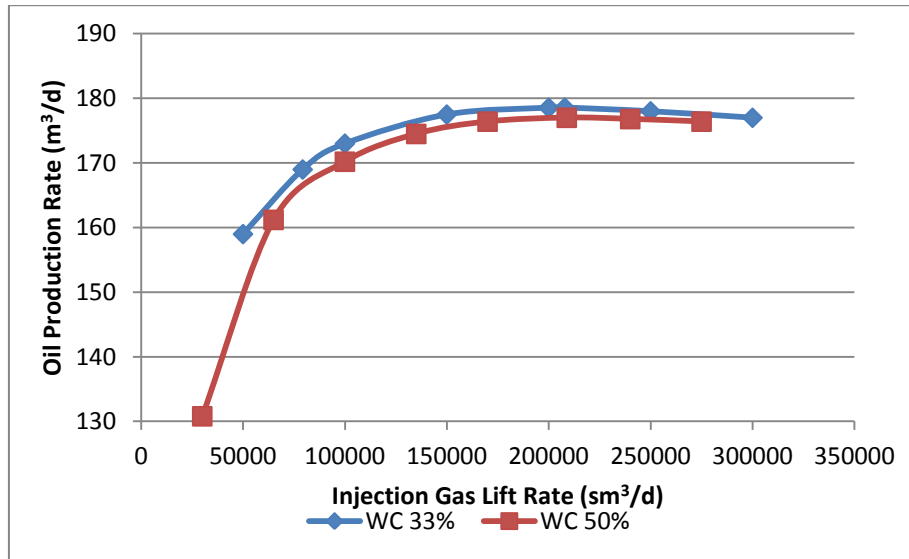


Figure B-7: Gas Lift Performance Curve for Well A-18

The economic optimum for well A-18 is located at 50000 sm<sup>3</sup>/d, which will allow to produce 160 m<sup>3</sup>/d. In the case of an increase in the water cut, the volume of gas needed to produce 160 m<sup>3</sup>/d of oil is 65000 sm<sup>3</sup>/d.

## v. Well A-19

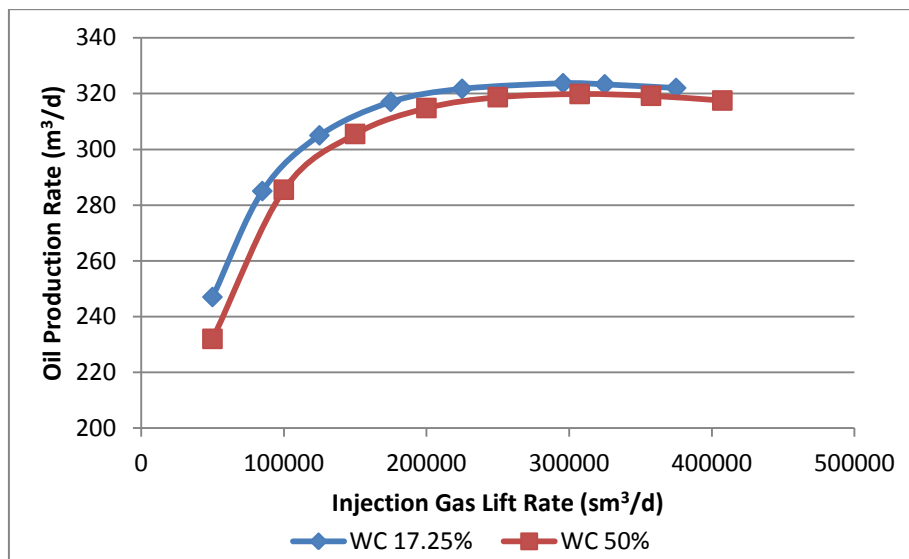


Figure B-8: Gas Lift Performance Curve for Well A-19

The economic optimum for well A-19 is located at 85000 sm<sup>3</sup>/d, which will allow to produce 285 m<sup>3</sup>/d. In the case of an increase in the water cut, the volume of gas needed to produce 285 m<sup>3</sup>/d of oil is 100000 sm<sup>3</sup>/d.

## vi. Well A-20

In the following figure it can be observed that the economic optimum for well A-20 is located at 85000  $\text{sm}^3/\text{d}$ , which will allow to produce 327  $\text{m}^3/\text{d}$ . In the case of an increase in the water cut from 46.86% to 85%, the volume of gas needed to produce 321  $\text{m}^3/\text{d}$  of oil is 95000  $\text{sm}^3/\text{d}$ .

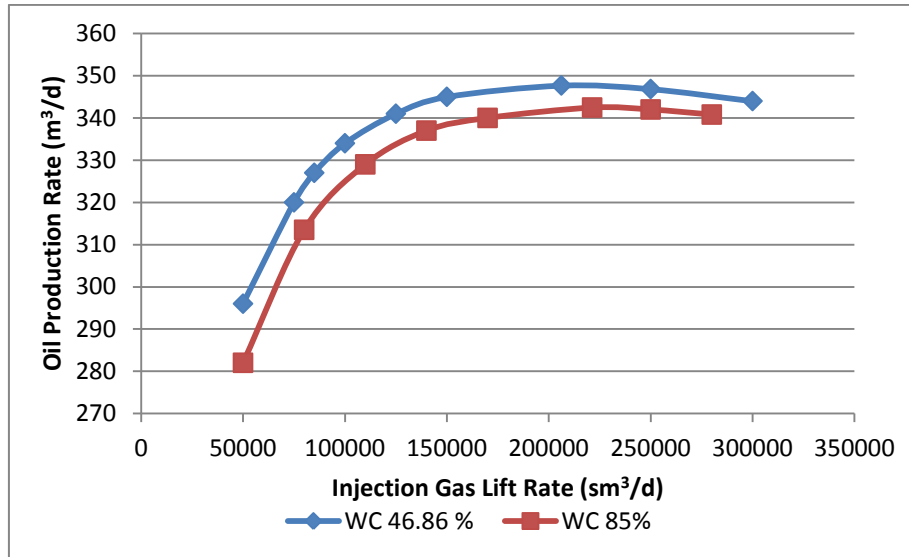


Figure B-9: Gas Lift Performance Curve for Well A-20

## vii. Well A-23

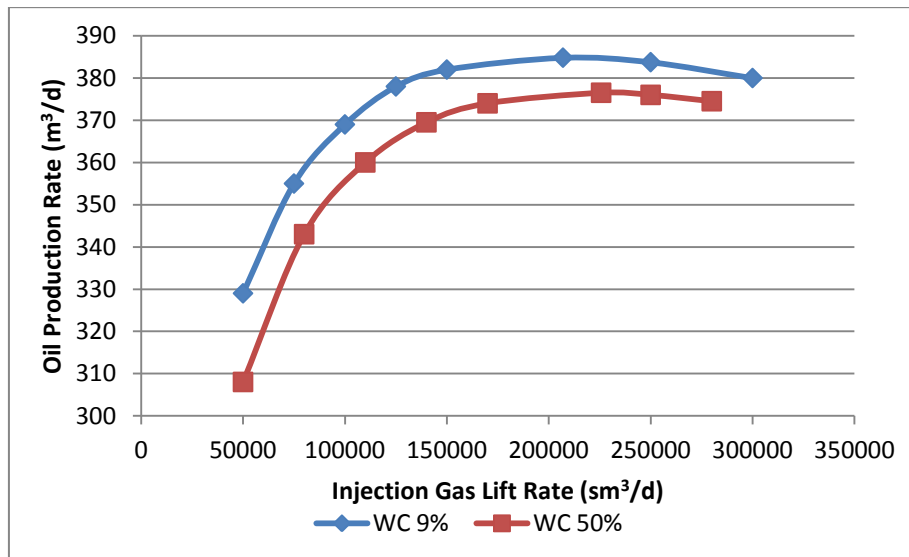


Figure B-10: Gas Lift Performance Curve for Well A-23

The economic optimum for well A-23 is located at 75000  $\text{sm}^3/\text{d}$ , which will allow to produce 355  $\text{m}^3/\text{d}$ . In the case of an increase in the water cut, the volume of gas needed to produce 360  $\text{m}^3/\text{d}$  of oil is 95000  $\text{sm}^3/\text{d}$ .



## viii. Well A-26

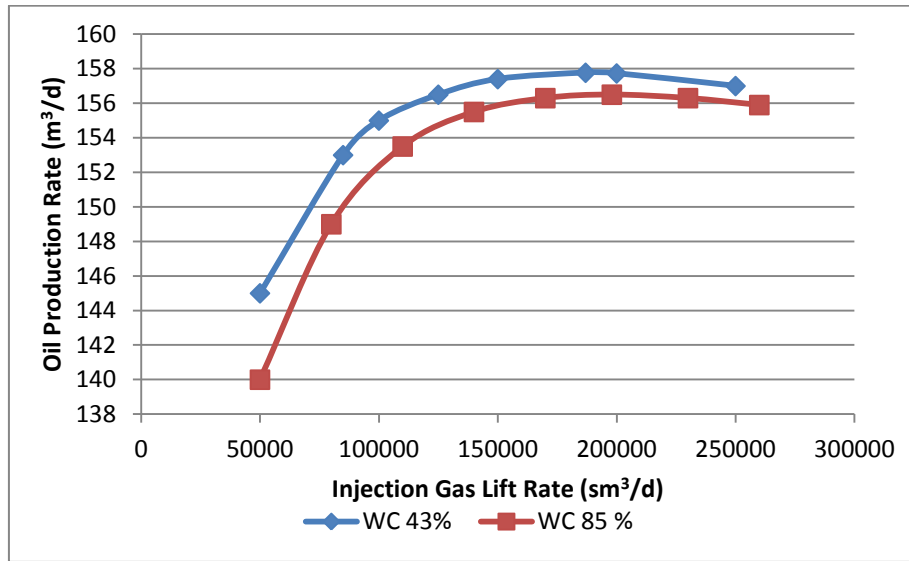


Figure B-11: Gas Lift Performance Curve for Well A-26

The economic optimum for well A-26 is located at 85000 sm<sup>3</sup>/d, which will allow to produce 153 m<sup>3</sup>/d. In the case of an increase in the water cut, the volume of gas needed to produce 151 m<sup>3</sup>/d of oil is 95000 sm<sup>3</sup>/d.

## ix. Well A-28

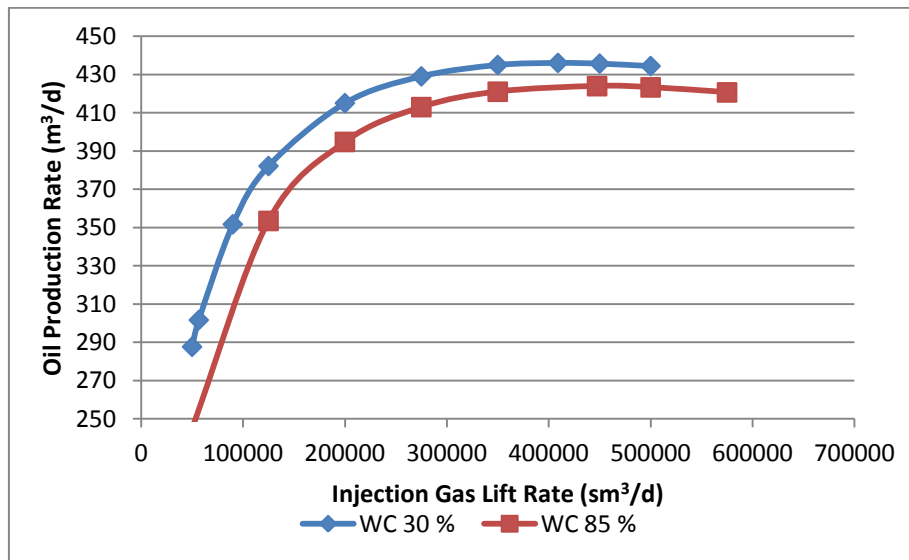


Figure B-12: Gas Lift Performance Curve for Well A-28

The economic optimum for well A-28 is located at 90000 sm<sup>3</sup>/d, which will allow to produce 351 m<sup>3</sup>/d. In the case of an increase in the water cut, the volume of gas needed to produce 353 m<sup>3</sup>/d of oil is 125000 sm<sup>3</sup>/d.

x. Well B-11

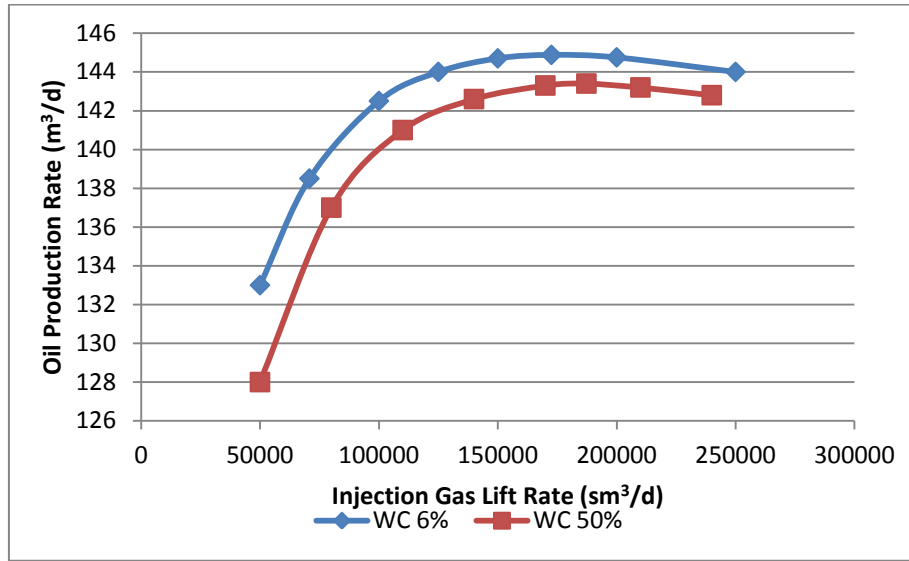


Figure B-13: Gas Lift Performance Curve for Well B-11

In the figure above it can be observed that the economic optimum for well B-11 is located at 70792 sm<sup>3</sup>/d, which will allow to produce 138 m<sup>3</sup>/d. In the case of an increase in the water cut from 6% to 50%, the volume of gas needed to produce 137 m<sup>3</sup>/d of oil is 80000 sm<sup>3</sup>/d.

xi. Well B-14

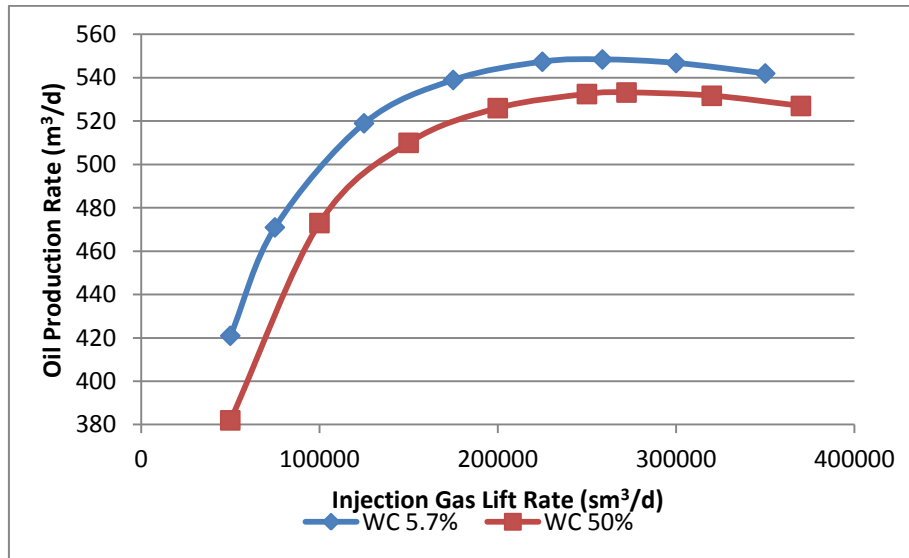


Figure B-14: Gas Lift Performance Curve for Well B-14

The economic optimum for well B-14 is located at 75000 sm<sup>3</sup>/d, which will allow to produce 471 m<sup>3</sup>/d. In the case of an increase in the water cut, the volume of gas needed to produce 470 m<sup>3</sup>/d of oil is 100000 sm<sup>3</sup>/d.

## xii. Well B-17

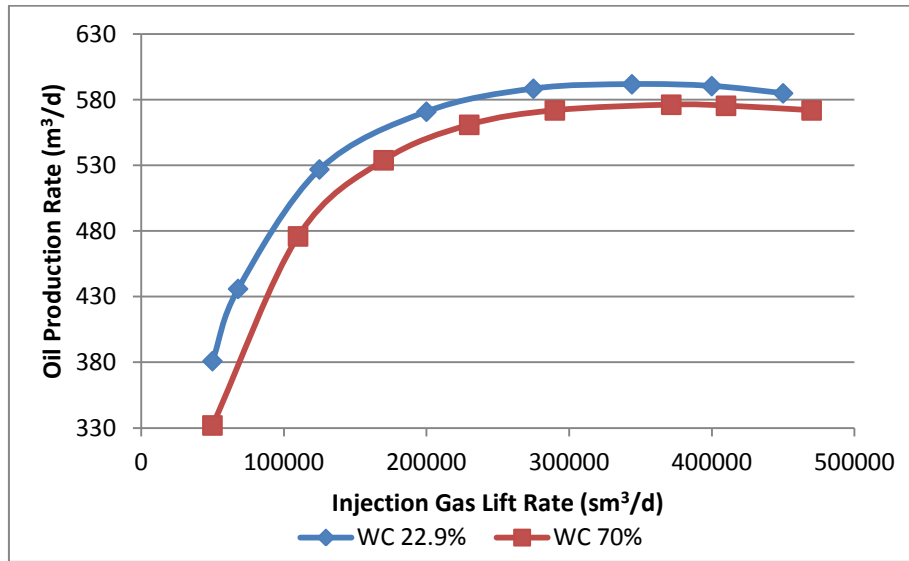


Figure B-15: Gas Lift Performance Curve for Well B-17

The economic optimum for well B-17 is located at 96480 sm<sup>3</sup>/d, which will allow to produce 481 m<sup>3</sup>/d. In the case of an increase in the water cut, the volume of gas needed to produce 476 m<sup>3</sup>/d of oil is 110000 sm<sup>3</sup>/d.

## xiii. Well B-19

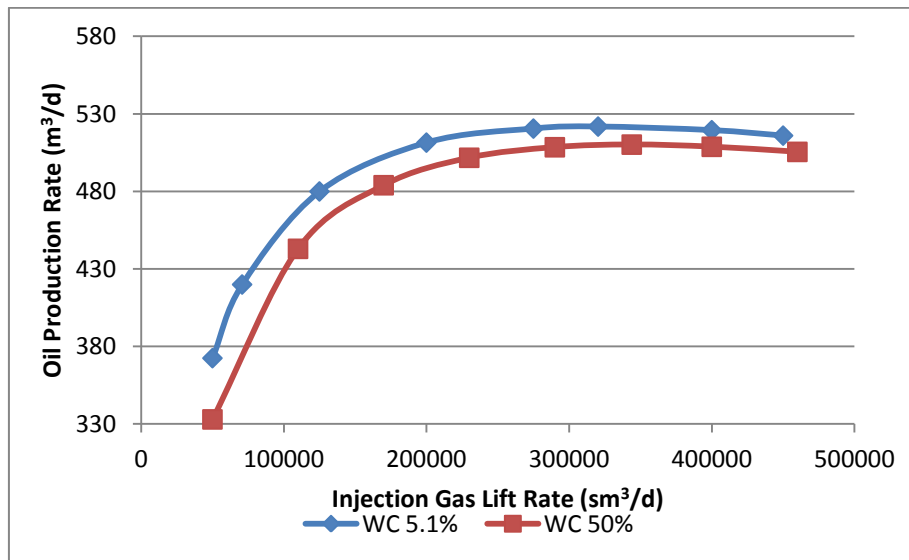


Figure B-16: Gas Lift Performance Curve for Well B-19

For the last well the economic optimum is located at 97896 sm<sup>3</sup>/d, which will allow to produce 450 m<sup>3</sup>/d. In the case of an increase in the water cut, the volume of gas needed to produce 443 m<sup>3</sup>/d of oil is 110000 sm<sup>3</sup>/d.